If new HCC nodules are detected with CTHA/CTAP, in addition to those detected with dynamic CT, the treatment of choice may be changed (15,16). For example, surgical resection and liver transplantation are usually contraindicated for multinodular HCC; that is, exceeding three nodules. Percutaneous tumor ablation methods, such as ethanol injection and microwave coagulation, have played an important role as nonsurgical treatments that can achieve high local cure rates without affecting background liver function (17–20). Radiofrequency ablation (RFA) is currently considered to be the most effective first-line percutaneous ablation protocol because of its greater efficacy in terms of local cure as compared with ethanol injection (21–24). However, even after complete ablation, patients frequently encounter intrahepatic tumor recurrence at a rate of 50% in 2 years, the majority of which occurs at locations distant from the primary ablated site (25). Considering the tumor doubling time, many nodules diagnosed as recurrent within 2 years were probably present at the time of first ablation. If nodules that are undetectable by conventional dynamic CT could be detected and ablated, the recurrence rate would be decreased.

Although CTHA/CTAP is one of the most sensitive techniques available for detection of small HCC, its disadvantages include invasiveness, high cost, and a high false-positive rate (26). The indication for CTHA/CTAP can be justified only when the expected benefits exceed the risk and cost of the procedure. We conducted a single-center, randomized, open-label, controlled trial to assess the utility of CTHA/CTAP before RFA in patients with early-stage HCC by comparing recurrence-free and overall survival.

METHODS

Patients

The study population consisted of patients with early-stage HCC with an indication for RFA. Those who met the following criteria were enrolled between September 2004 and February 2009: (i) diagnosis of typical HCC on dynamic CT performed within 2 weeks, i.e., hyperattenuation during the arterial phase and hypoattenuation during the equilibrium phase (5,6); (ii) tumor size ≤3.0 cm and no more than three tumor nodules; (iii) Child-Pugh class A liver function; and (iv) age >20 years. Exclusion criteria were: allergy to contrast media; portal or hepatic vein tumor thrombosis; extrahepatic metastasis; diffuse and infiltrative tumors; renal failure (serum creatinine >2.0 mg/dl, or serum urea nitrogen >30 mg/dl); impaired coagulation (e.g., platelet count $<50 \times 10^3/\mu l$, or prothrombin activity <50%); pregnancy; or past history of choledochojejunostomy. We included those with previous treatments as well as treatment-naive cases provided that there was no local recurrence at enrollment. These inclusion criteria and the study design did not change till the study completely ended. The study design conformed to the Declaration of Helsinki Principles and was approved by the ethics committee of our institution. The study was registered at the University Hospital Medical Information Network (UMIN) Clinical Trial Registry (UMIN-CTR000000070). Written informed consent was obtained from each patient. This study complied with the CONSORT guidelines for reporting of clinical trials (27).

Study design

Before receiving RFA, patients were randomly assigned to undergo CTHA/CTAP or not in equal numbers. Patient registration and randomization were performed by computer-generated allocation at a web-based data center (Internet Data and Information Center for Medical Research) administered by UMIN. At the time of randomization, patients were stratified either as treatment naive, for whom RFA was planned as an initial treatment for HCC, or recurrent, for whom RFA was planned for recurrent HCC. The randomization was based on the Efron's biased-coin design (28). In principal, the assignment was not blinded to the investigators and the participants. The interval between random assignment and implementation of treatment for HCC was <4 weeks. CTHA/CTAP was performed on the assigned patients on the second day of admission, and RFA was performed 2 or 3 days later, given that the total number of HCC nodules remained <4. When ≥4 HCC nodules were detected on CTHA/CTAP, patients first received transarterial chemoembolization (TACE) immediately after CTHA/CTAP, followed later by RFA to achieve complete ablation of the tumor nodules.

Radiographic procedures

For the diagnosis of HCC at study entry, intravenous contrast-enhanced dynamic CT was performed on an outpatient basis using an X-ray CT device with 4, 8, or 16 detector rows (Aquilion 4/16; Toshiba, Tokyo, Japan; LightSpeed Qx/I, LightSpeed Ultra; GE Healthcare, Milwaukee, WI). Images were obtained during the early arterial, late arterial, and equilibrium phases at 28, 40, and 120 s after starting the intravenous bolus injection of iopamidol (Iopamiron; Nihon Schering, Osaka, Japan) or iohexol (Omnipaque; Daiichi Sankyo, Tokyo, Japan) at a rate of 2.3–3.3 ml/s with a power injector. The total dose of iodine was 0.7 g/kg body weight, with an upper limit of 37 g iodine. The injection time for the contrast material was 30 s. Images were reconstructed with a section thickness of 2.5 mm and a reconstruction interval of 1.5 mm, and were reviewed by experienced radiologists.

CTHA/CTAP was performed on an inpatient basis. First, a 4-Fr modified Shepherd-hook catheter and a 4-Fr hepatic-curve catheter were placed in the celiac artery and superior mesenteric artery, respectively, through bilateral femoral arteries, according to Seldinger's method. Digital subtraction angiography was performed from the celiac artery to evaluate hepatic artery anatomy. A microcatheter was inserted through the 4-Fr catheter and placed in the proper or common hepatic artery for hepatic arteriography.

The CTAP catheter was placed in the superior mesenteric artery in all cases. In the case of a replaced or accessory right hepatic artery, the catheter was inserted well beyond the origin of the hepatic artery to prevent contrast medium overflow into the hepatic artery. Less than 30 ml of contrast agent, which was diluted to 100 mg I/ml, was used before the CTHA/CTAP study. First, CTAP was performed using 90 ml nonionic contrast medium diluted to 100 mg I/ml, and then CT scanning was performed 30 s after the start of the injection at a rate of 3.0 ml/s. Multidetector-row CT images were obtained during a single breath hold in a longitudinal direction with collimation of 1 mm, table speed of 30 mm/s, 120 kVp, and

300 mAs. CTHA was performed at least 5 min after CTAP, using the same parameters. CT scanning was performed at 10 and 45 s after the start of contrast medium injection into the microcatheter at a rate of 2.0–2.5 ml/s. A total of 30–50 ml contrast agent diluted to 100 mg I/ml was used. When the liver was perfused by two or more hepatic arteries such as a replaced right hepatic artery, accessory right hepatic artery, or left hepatic artery downstream of the left gastric artery, CTHA was performed from each of the respective arteries. A diagnosis of typical HCC on CTHA/CTAP was defined as a round hypervascular nodule on CTHA with a defect on CTAP, accompanied by corona enhancement during the second phase of CTHA or hypoattenuation during the equilibrium phase of prior dynamic CT (10,29).

TACE was additionally performed when ≥4 HCC nodules were detected on CTHA/CTAP, as evaluated at the time by the operating radiologist. The procedure used 3.0 ml contrast medium, 30 mg doxorubicin (Adriacin; Kyowahakko Kirin, Tokyo, Japan), and 3.0 ml iodized oil (Lipiodol Ultra-Fluid; Guerbet Japan, Tokyo, Japan). The amounts of contrast medium and iodized oil in this suspension were arbitrarily adjusted according to tumor size. This agent was injected into each feeder of the HCC, followed by infusion of 2-mm-diameter gelatin sponge particles (Gelpart; Nihonkayaku, Tokyo, Japan).

CTHA/CTAP images were scrutinized by two experienced radiologists, who made the final diagnosis. The radiologists were not blinded to information regarding the preceding conventional dynamic CT. Preceding intravenous contrast-enhanced dynamic CT was retrospectively reviewed for nodules newly diagnosed by CTHA/CTAP to determine whether the nodules could have been detected on dynamic CT.

Radiofrequency ablation

RFA was performed on an inpatient basis. The precise procedure of RFA is described elsewhere (30). All RFA procedures were performed percutaneously under ultrasonographic guidance. We used a 17-gauge cooled-tip electrode (Cool-Tip; RF Ablation System, Covidien, Boulder, Colombia, CO) for RFA. Radiofrequency energy was delivered for 6–12 min for each application. For large tumors, the electrode was repeatedly inserted into different sites, such that the entire tumor could be enveloped by assumed necrotic volumes. A CT scan with a 5-mm section thickness was performed 1–3 days after RFA to evaluate technical effectiveness. Complete ablation was defined as hypoattenuation of the entire tumor. We intended to ablate not only the tumor but also some of the liver parenchyma surrounding it. When we suspected that some portion of tumor remained nonablated, RFA was repeated. We did not predefine the procedure number in a treatment: treatment was generally continued until CT imaging demonstrated necrosis of the entire tumor.

Follow-up

The follow-up regimen after RFA consisted of blood tests and monitoring of tumor markers in an outpatient setting. Ultrasonography and dynamic CT were performed every 4 months. Tumor recurrence was defined as a newly developed lesion on a dynamic CT that showed hyperattenuation in the arterial phase with washout in the late phase. Recurrent site was categorized as intrahepatic recurrence distant from ablated nodules, local tumor progression defined as the appearance of viable cancer tissue touching the ablated nodules, and extrahepatic metastasis (31). The follow-up was censored in February 2011 when 2 years had passed after the enrollment of patient 280. No interim analysis was specified in the protocol.

End points

The primary end point was recurrence-free survival, where both recurrence and death were treated as an event. We intended to ablate all detected nodules in both groups. When additional nodules were detected by CTHA/CTAP, the newly detected nodules were also ablated. When >3 nodules were diagnosed as HCC by CTHA/CTAP, we performed TACE and subsequently intended to ablate all of the nodules. When nonablated viable tumors were detected by CT for treatment evaluation, those cases were treated as an event 120 days after randomization. Even when newly detected nodules showed dense Lipiodol deposits after TACE, the nodules were considered as viable if the nodules were nonablated.

Secondary end points were the number of additional nodules detected by CTHA/CTAP, the proportion of patients with complete ablation, overall survival, and safety of CTHA/CTAP and RFA. Complications were defined according to the guidelines of the Society of Interventional Radiology (32). According to the guidelines, major complications were defined as those that required therapy or prolonged hospitalization, or left permanent adverse sequelae, or death.

Statistical analysis

This study was designed to detect a 15% increase in 2-year recurrence-free survival in the CTHA/CTAP group from an anticipated 35% in the control group. To detect this difference with a power of 80% and type I error of 5% (two-sided test), we needed 280 patients (140 for each arm). Differences between groups for each characteristic were tested for significance with Fisher's exact test for categorical variables and t-test for continuous variables. All data necessary for analysis was corrected in the main computer server system of University of Tokyo, Department of Gastroenterology.

Recurrence-free survival and overall survival were calculated using the Kaplan–Meier method and were compared by the log-rank test. Cox proportional hazard regression was used to calculate hazard ratios with 95% confidence interval (CI) between the groups in univariate and multivariate settings. The primary end point was evaluated in subgroups according to the following characteristics: age, sex, body mass index, treatment naivety, hepatitis B surface antigen (HBsAg) positivity, hepatitis C virus antibody positivity, tumor size, tumor number, platelet count, tumor marker positivity for α-fetoprotein (AFP), lens culinaris agglutinin-reactive fraction of AFP, and des-γ-carboxy prothrombin. An adjusted hazard ratio comparing the groups was calculated using multivariate Cox regression with factors that showed significance
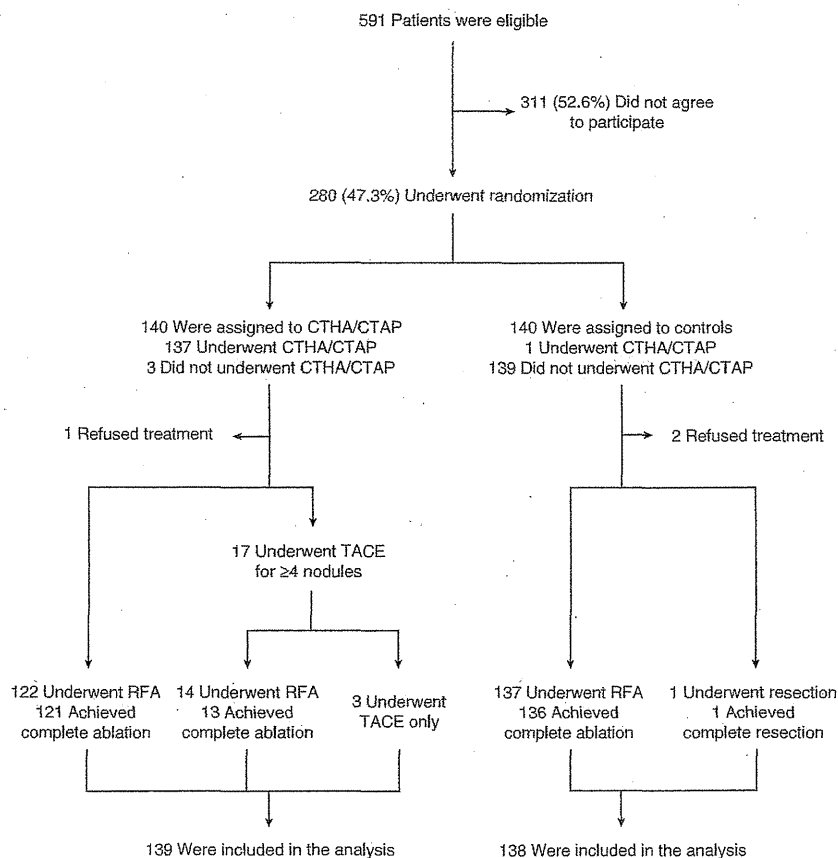
Figure 1. Patient enrollment and outcomes. CTAP, computed tomography during arterial portography; CTHA, computed tomography during hepatic arteriography; RFA, radiofrequency ablation; TACE, transarterial chemoembolization.

in univariate analysis. Data at entry were used for the analyses. A *post hoc* analysis comparing the recurrence-free survival of those with and without newly diagnosed HCC in the CTHA/CTAP group was performed.

All analyses were performed on an intention-to-treat basis. Differences with a two-sided *P* value of <0.05 were considered statistically significant. Data processing and analysis were performed with S-PLUS ver. 7 (TIBCO Software, Palo Alto, CA). Finally, all authors had access to the study data and had reviewed and approved the final manuscript.

RESULTS

Patient enrollment

According to the study protocol, the registration started from September 2004 for 5 years and the follow-up was censored in February 2011 when 2 years had passed after the enrollment of patient 280. During the study period, 280 of 591 (47.4%) eligible patients agreed to participate in the trial, and 140 of these were randomly assigned to undergo CTHA/CTAP before RFA. Three patients declined to undergo CTHA/CTAP after assignment. A total of 140 patients were randomly assigned to the control

group. One patient assigned to the control group received CTHA/CTAP because of strong preference (**Figure 1**).

Treatment

In 45 (32.4%) patients, 75 nodules with a median diameter of 8 mm (range, 2–20) were additionally diagnosed by experienced radiologists as definite HCC on CTHA/CTAP. The detailed characteristics of newly diagnosed nodules have been reported previously (33). In 17 patients, the number of HCC nodules exceeded 3 after CTHA/CTAP, and TACE was performed subsequently. We intended to ablate all nodules by RFA including additionally detected nodules. In 122 patients, there were ≤3 HCC nodules, and complete ablation was obtained in 121 patients (99.2%). Among 17 patients treated with TACE, 14 (82.4%) subsequently underwent RFA and complete ablation was obtained in 13 (92.9%) patients. The remaining 3 patients (17.6%) did not undergo RFA because of tumor nodule multiplicity in 2 patients and simultaneously diagnosed malignant B-cell lymphoma in the third patient. Among 140 patients who were assigned to the control group, 137 (97.9%) were treated with RFA, and complete ablation was obtained in 136 (99.3%) patients. One patient withdrew consent and underwent hepatic resection. Two patients refused to receive

Table 1. Baseline characteristics of the patients[a]

Characteristics	CTHA/CTAP (N=139)	Control (N=138)	P value
Age, years	70 (63–74)	70 (64–75)	0.43
Male; n (%)	93 (67)	86 (62)	0.42
Alcohol >80 g/day, n (%)	23 (17)	20 (15)	0.82
BMI (kg/m²)	23.1 (21.4–25.1)	23.4 (21.2–25.3)	0.48
Viral markers			
HCVAb positive, n (%)	104 (75)	99 (72)	0.59
HBsAg positive, n (%)	21 (15)	20 (14)	1
Serum albumin (g/dl)	3.8 (3.6–4.1)	3.9 (3.6–4.1)	0.20
Total bilirubin (mg/dl)	0.8 (0.6–1.0)	0.8 (0.6–1.0)	0.31
AST (IU/l)	56 (34–69)	57 (33–70)	0.84
ALT (IU/l)	54 (29–63)	57 (27–73)	0.61
Platelet count (×10³/µl)	128 (89–163)	130 (91–159)	0.88
Prothrombin activity (%)	80 (72–90)	81 (74–87)	0.39
Treatment-naive case, n (%)	77 (55)	74 (54)	0.81
Previously treated case, n (%)	62 (45)	64 (46)	
Resection, n (%)[b]	15 (24)	16 (25)	0.27
RFA, n (%)[b]	46 (74)	45 (70)	
Ethanol injection, n (%)[b]	10 (16)	3 (4.6)	
TACE, n (%)[b]	11 (18)	7 (11)	
Tumor size (cm)	1.6 (1.2–2.0)	1.7 (1.2–2.0)	0.91
Single nodule, n (%)	101 (73)	98 (71)	0.76
AFP >100 ng/ml, n (%)	23 (17)	24 (17)	0.85
DCP >100 mAU/ml, n (%)	16 (12)	22 (16)	0.28
AFP-L3 >15%, n (%)	16 (12)	15 (11)	0.86

AFP, α-fetoprotein; AFP-L3, lens culinaris agglutinin-reactive fraction of AFP; ALT, alanine aminotransferase; AST, aspartate aminotransferase; BMI, body mass index; CTHA/CTAP, computed tomography during hepatic arteriography and arterial portography; DCP, des-γ-carboxy prothrombin; HBsAg, hepatitis B surface antigen; HCVAb, hepatitis C virus antibody; RFA, radiofrequency ablation, TACE, transarterial chemoembolization.
[a]Data are expressed as median (25th–75th percentiles) or number (percent).
[b]Including overlap.

any treatment and were lost to follow-up. Finally, 139 (99.3%) patients in the CTHA/CTAP group and 138 (98.6%) patients in the control group were included in the analysis.

Patient characteristics

There was no statistically significant difference in patient characteristics between the groups (**Table 1**). Median age at enrollment was 70 years, and approximately two-thirds of patients were male. Approximately 55% of patients were treatment-naive cases and the remaining patients had a history of previous treatment. Among those previously treated patients, the median interval between the initial treatment and the study enrollment was 42 (interquartile range, 22–65) months in the CTHA/CTAP group and 30 (20–61)

months in the control group. There was no statistically significant difference between the two groups (P=0.72). The total number of HCC nodules detected in original contrast-enhanced dynamic CT was 197 (101 patients were uninodular and the rest were multinodular) in the CTHA/CTAP group and 196 (98 patients were uninodular and the rest were multinodular) in the control group.

Recurrence

By the end of the follow-up, tumor recurrence was identified in 109 patients (78.4%) in the CTHA/CTAP group and 112 patients (81.2%) in the control group. The distribution of recurrent site was intrahepatic distant recurrence (N=98), local tumor progression (N=7), both (N=1), and extrahepatic metastasis (N=3) in the CTHA/CTAP group and intrahepatic distant recurrence (N=103), local tumor progression (N=4), both (N=2), and extrahepatic metastasis (N=3) in the control group. Five patients (3.6%) in the CTHA/CTAP group and 1 patient (0.7%) in the control group in whom complete ablation could not be obtained by RFA were treated as recurrence on 120 days after randomization when the first follow-up CT would have been scheduled. In each group, four patients died without recurrence. The cumulative recurrence-free survival rates at 1, 2, and 3 years were 60.1, 29.0, and 18.9% in the CTHA/CTAP group and 52.2, 29.7, and 23.1% in the control group, respectively (**Figure 2a**). The difference between the two groups was not statistically significant (P=0.66 by log-rank test; hazard ratio, 0.94 for CTHA/CTAP vs. control; 95% CI, 0.73–1.22). The CTHA/CTAP group showed better recurrence-free survival with marginal statistical significance in the subgroups with higher AFP or AFP-L3 values (**Figure 3**).

Univariate Cox regression analysis identified older age (P=0.01), hepatitis C virus antibody positivity (P=0.001), lower albumin level (P=0.04), recurrent cases (P<0.001), multinodular HCC (P<0.001), and higher AFP level (P=0.02) as significant predictors for recurrence-free survival (**Table 2**). Adjusted hazard ratio of the CTHA/CTAP group vs. the control group by multivariate Cox regression analysis was 0.86 (95% CI, 0.67–1.12; P=0.27, **Table 3**).

Overall survival

By the end of the follow-up, 51 patients (36.7%) in the CTHA/CTAP group and 45 patients (32.6%) in the control group died. The cumulative overall survival rates at 3 and 5 years were 79.7 and 56.4% in the CTHA/CTAP group and 86.8 and 60.1% in the control group, respectively (**Figure 2b**). There was no statistically significant difference between the groups (P=0.50 by log-rank test; hazard ratio, 1.15, 95% CI, 0.77–1.71).

Safety

No procedural complications attributable to CTHA/CTAP or TACE were observed. Major complications related to RFA were observed in 2 patients (1.4%) in the CTHA/CTAP group (2 with neoplastic seeding) and in 3 patients (2.2%) in the control group (1 each with hepatic infarction, hemothorax, and neoplastic seeding). There was no procedure-related death.
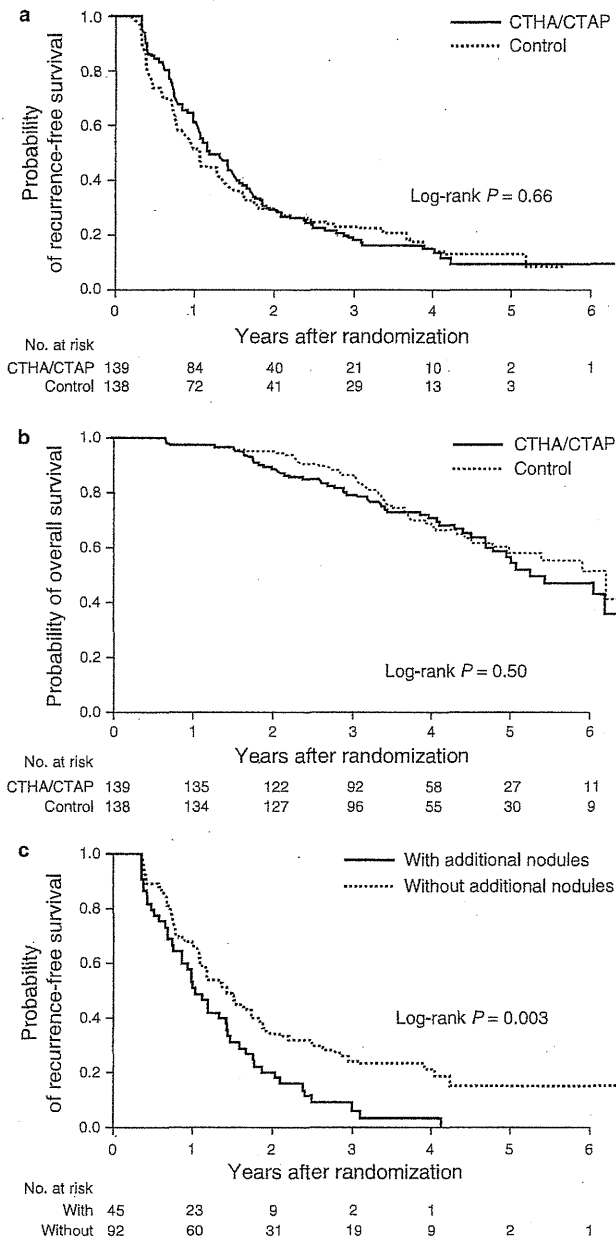
Subgroup	N	Hazard ratio (95%CI)		P value
All patients	277	0.94	(0.73–1.22)	0.66
Age				
≥69 yr	150	1.00	(0.71–1.42)	0.99
<69 yr	127	0.90	(0.61–1.33)	0.61
Sex				
Male	179	0.94	(0.68–1.29)	0.71
Female	98	0.95	(0.61–1.48)	0.83
BMI (kg/m²)				
>25	76	1.01	(0.62–1.66)	0.96
≤25	201	0.92	(0.68–1.25)	0.61
Treatment-naive case				
Yes	151	1.06	(0.73–1.54)	0.74
No	126	0.78	(0.55–1.12)	0.18
HBsAg				
Positive	41	1.02	(0.78–1.35)	0.87
Negative	246	0.68	(0.32–1.44)	0.31
HCVAb				
Positive	203	0.72	(0.41–1.25)	0.24
Negative	73	1.05	(0.79–1.41)	0.72
Tumor size (cm)				
≤2	218	0.92	(0.69–1.23)	0.57
>2	59	1.00	(0.55–1.79)	0.99
Tumor number				
Single	199	1.01	(0.74–1.38)	0.94
Multiple	78	0.82	(0.52–1.29)	0.38
Platelet (×10⁹/l)				
>12	142	0.91	(0.63–1.31)	0.60
≤12	135	0.94	(0.65–1.35)	0.72
AFP (ng/ml)				
>100	47	0.61	(0.33–1.12)	0.11
≤100	230	1.03	(0.78–1.37)	0.84
AFP-L3				
>15%	31	0.50	(0.23–1.08)	0.08
≤15%	246	1.02	(0.77–1.34)	0.91
DCP (mAU/ml)				
>100	38	0.81	(0.39–1.70)	0.58
≤100	238	0.98	(0.74–1.29)	0.88

Figure 3. Recurrence-free survival of subgroups by Cox proportional hazard regression according to clinical characteristics at study entry. AFP, α-fetoprotein; BMI, body mass index; CI, confidence interval; CT, computed tomography; CTAP, computed tomography during arterial portography; CTHA, computed tomography during hepatic arteriography; DCP, des-γ-carboxy prothrombin; HBsAg, hepatitis B surface antigen; HCVAb, hepatitis C virus antibody; yr, year.

Figure 2. Kaplan–Meier estimate of the recurrence-free survival and overall survival. (a) The cumulative recurrence-free survival rates at 1, 2, and 3 years were 60.1, 29.0, and 18.9% in the CTHA/CTAP group and 52.2, 29.7, and 23.1% in the control group, respectively. (b) The cumulative overall survival rates at 3 and 5 years were 79.7 and 56.4% in CTHA/CTAP group and 86.8 and 60.1% in the control group, respectively. (c) Patients with an additional nodule detected by CTHA/CTAP showed significantly poorer recurrence-free survival than those without an additional nodule. CTAP, computed tomography during arterial portography; CTHA, computed tomography during hepatic arteriography.

Recurrence-free survival between those with and without additional nodules in CTHA/CTAP group

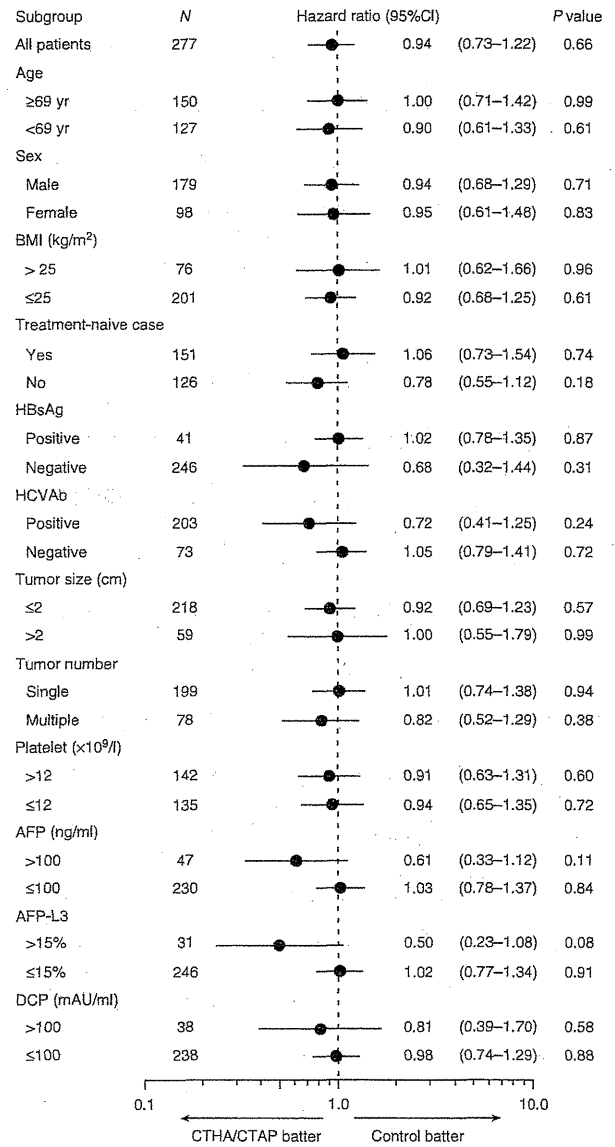As a *post hoc* analysis, we compared the recurrence-free survival between those with ($N=45$) and without ($N=92$) additional HCC nodules diagnosed by CTHA/CTAP. As compared with those in whom additional HCC nodules were not detected by CTHA/CTAP, those with additional nodules included more HBsAg-negative patients (97.7 vs. 78.3%, $P=0.002$), previously treated patients (62.2 vs. 23.9%, $P=0.006$), and patients with multiple HCC nodules on dynamic CT (44.4 vs. 17.4%, $P=0.002$). Patients with additional nodule by CTHA/CTAP showed significantly poorer

Table 2. Univariate Cox's proportional hazard regression analysis of the risk for recurrence-free survival

Variable	Hazard ratio (95% CI)	P value
CTHA/CTAP vs. control	0.94 (0.73–1.22)	0.66
Age (per year)	1.02 (1.00–1.04)	0.01
Female vs. male	1.02 (0.78–1.34)	0.88
Alcohol >80 g/day	1.02 (0.88–1.17)	0.81
HCVAb positive	1.69 (1.23–2.31)	0.001
BMI (per 1.0 kg/m²)	1.02 (0.98–1.06)	0.35
Albumin (per 1.0 g/dl)	0.72 (0.52–0.98)	0.04
Total bilirubin (per 1.0 mg/dl)	1.02 (0.97–1.07)	0.51
AST >40 IU/l	1.14 (0.99–1.31)	0.07
ALT >40 IU/l	1.05 (0.92–1.20)	0.45
Platelet count >10×10³/µl	0.89 (0.78–1.01)	0.08
Recurrent case	2.33 (1.79–3.02)	<0.001
Tumor size of maximal nodule >2.0 cm	0.97 (0.85–1.10)	0.62
Multinodular	1.38 (1.20–1.59)	<0.001
AFP >100 ng/ml	1.21 (1.03–1.43)	0.02
DCP >100 mAU/ml	0.99 (0.82–1.20)	0.93
AFP-L3 >15%	1.20 (0.99–1.46)	0.07

AFP, α-fetoprotein; AFP-L3, lens culinaris agglutinin-reactive fraction of AFP; ALT, alanine aminotransferase; AST, aspartate aminotransferase; BMI, body mass index; CI, confidence interval; CTHA/CTAP, computed tomography during hepatic arteriography and arterial portography; DCP, des-γ-carboxy prothrombin; HCVAb, hepatitis C virus antibody.

Table 3. Multivariate Cox's proportional hazard regression analysis of the risk for recurrence-free survival

Variable	Hazard ratio (95% CI)	P value
CTHA/CTAP vs. control	0.86 (0.0.67–1.12)	0.27
Age (per year)	1.01 (0.99–1.02)	0.36
HCVAb positive	1.36 (0.98–1.89)	0.07
Albumin (per 1.0 g/dl)	0.75 (0.53–1.07)	0.11
Recurrent case	2.21 (1.69–2.89)	<0.001
Multinodular	1.69 (1.27–2.25)	<0.001
AFP >100 ng/ml	1.41 (0.996–1.98)	0.052

AFP, α-fetoprotein; CI, confidence interval; CTHA/CTAP, computed tomography during hepatic arteriography and arterial portography; HCVAb, hepatitis C virus antibody.

recurrence-free survival than those without additional nodules (P = 0.003, **Figure 2c**).

DISCUSSION

An advance in diagnostic technology generally indicates improved sensitivity or specificity, which corresponds to the detection of smaller lesions with a clearer view in imaging modalities. In our previous study, we showed that 75 nodules with a mean diameter of 8.7 mm (range, 2–20 mm) in 45 (33%) of 139 patients who underwent CTHA/CTAP were additionally diagnosed as definite HCC, compared with dynamic CT examination (33). However, no significant difference was observed in terms of recurrence-free survival between those who did and did not undergo CTHA/CTAP before RFA.

One reason for this discrepancy may be that the impact of CTHA/CTAP on recurrence reduction was diluted by a long-term follow-up of >2 years. It is unlikely that CTHA/CTAP could detect small nodules that would be detected ≥2 years later by conventional dynamic CT. In fact, the number of recurrences identified within 1 year after enrollment was lower in the CTHA/CTAP group than the control group (54 vs. 65, data not shown).

Another reason could be that fewer patients achieved complete ablation of target nodules in the CTHA/CTAP group than in the control group. The additionally diagnosed HCC nodules were small, and detection of these nodules by ultrasonography was difficult. Recent technologies such as contrast ultrasonography or fusion imaging, which can improve the accuracy of ablation techniques (34–36), may increase the probability of detection of smaller nodules before RFA.

Precise evaluation of the stage of progression is important for deciding on treatment procedures in HCC management. Seventeen patients in the CTHA/CTAP group were diagnosed with ≥4 nodules by CTHA/CTAP, which is not considered suitable for RFA according to widely used criteria.

In our previous study, we showed that recurrence as opposed to initial occurrence, multinodularity on dynamic CT, and HBsAg negativity were significant predictors for finding additional HCC by CTHA/CTAP (33). In fact, the CTHA/CTAP group showed better outcomes in the subgroups with HBsAg-negative cases, previously treated patients, and multinodular HCC. However, post hoc analysis comparing recurrence-free survival of those with and without additional nodules detected by CTHA/CTAP showed that those with a higher probability of additional nodules were also at a higher risk of recurrence. The advantage of CTHA/CTAP in finding more HCC nodules might be counter balanced by the higher risk of recurrence.

This study has several limitations. First, the additional nodules detected by CTHA/CTAP were not confirmed histologically. Therefore, we cannot exclude the possibility of overdiagnosis. Second, 45% of the patients had a history of previous treatment including resection, RFA, and TACE. Those previous treatments might substantially alter the hemodynamic status in the liver and affect the accuracy of CTHA/CTAP. On the other hand, in the previously treated cases, the radiologists could refer to the past series of dynamic CT during performing CTHA/CTAP, which might improve the accuracy of CTHA/CTAP as compared with treatment-naive cases. Third, 17 patients in the CTHA/CTAP group underwent TACE as a salvage treatment because total number of HCC nodules exceeded 3 after CTHA/CTAP. This might affect the recurrence-free and overall survival in the CTHA/CTAP group.

Our results may be extrapolated to other imaging modalities including gadoxetic acid–enhanced magnetic resonance imaging and second-generation contrast ultrasonography (37,38). These newly developed modalities also make possible the detection of small nodules that are invisible by dynamic CT. However, better diagnosis does not necessarily lead to better primary outcome.

In conclusion, CTHA/CTAP before RFA resulted in improved HCC diagnosis and detection of additional nodules in one-third of the study participants. However, it did not improve recurrence-free survival. The indications for CTHA/CTAP should be evaluated carefully.

Study protocol URL: https://upload.umin.ac.jp/cgi-open-bin/ctr/ctr.cgi?function=brows&action=brows&recptno=R000000117&type=summary&language=E.

CONFLICT OF INTEREST

Study Highlights

WHAT IS CURRENT KNOWLEDGE

✓ Computed tomography with hepatic arteriography and arterial portography (CTHA/CTAP) give higher hepatocellular carcinoma (HCC) detection sensitivity than conventional dynamic enhanced CT.

✓ CTHA/CTAP is an invasive procedure requiring the insertion of an intraarterial catheter through a femoral puncture.

✓ The indication for CTHA/CTAP can be justified only when the expected benefits exceed the risks and cost of the procedure.

WHAT IS NEW HERE

✓ Our study is the first randomized controlled trial (RCT) to evaluate the utility of CTHA/CTAP before radiofrequency ablation (RFA) in patients with HCC in the whole world.

✓ The best candidates for CTHA/CTAP were patients with multinodular HCC, and recurrent cases after previous treatment.

✓ However, CTHA/CTAP before RFA did not improve cumulative recurrence-free survival or overall survival.

✓ These observations are clinically important as the technique had limited utility and highlights the observation that patient outcomes are probably not related to the presence of small liver nodules.

✓ These findings reinforce the notion of genetic determinants of HCC recurrence.

REFERENCES

1. El-Serag HB, Mason AC. Rising incidence of hepatocellular carcinoma in the United States. N Engl J Med 1999;340:745–50.
2. Kiyosawa K, Umemura T, Ichijo T *et al.* Hepatocellular carcinoma: recent trends in Japan. Gastroenterology 2004;127:S17–26.
3. Itai Y, Matsui O. Blood flow and liver imaging. Radiology 1997;202:306–14.
4. Matsui O. Detection and characterization of hepatocellular carcinoma by imaging. Clin Gastroenterol Hepatol 2005;3:S136–40.
5. Teratani T, Yoshida H, Shiina S *et al.* A novel display of reconstruction computed tomography for the detection of small hepatocellular carcinoma. Liver Int 2004;24:619–24.
6. Fujishima T, Yoshida H, Obi S *et al.* Analysis of factors influencing hepatocellular carcinoma detection: efficient use of computed tomography during arterial portography and during hepatic arteriography. J Gastroenterol 2005;40:266–73.
7. Sangiovanni A, Manini MA, Iavarone M *et al.* The diagnostic and economic impact of contrast imaging techniques in the diagnosis of small hepatocellular carcinoma in cirrhosis. Gut 2010;59:638–44.
8. Murakami T, Oi H, Hori M *et al.* Helical CT during arterial portography and hepatic arteriography for detecting hypervascular hepatocellular carcinoma. AJR Am J Roentgenol 1997;169:131–5.
9. Kanematsu M, Hoshi H, Imaeda T *et al.* Detection and characterization of hepatic tumors: value of combined helical CT hepatic arteriography and CT during arterial portography. AJR Am J Roentgenol 1997;168:1193–8.
10. Irie T, Takeshita K, Wada Y *et al.* CT evaluation of hepatic tumors: comparison of CT with arterial portography, CT with infusion hepatic arteriography, and simultaneous use of both techniques. AJR Am J Roentgenol 1995;164:1407–12.
11. Small WC, Mehard WB, Langmo LS *et al.* Preoperative determination of the resectability of hepatic tumors: efficacy of CT during arterial portography. AJR Am J Roentgenol 1993;161:319–22.
12. Soyer P, Levesque M, Elias D *et al.* Detection of liver metastases from colorectal cancer: comparison of intraoperative US and CT during arterial portography. Radiology 1992;183:541–4.
13. Soyer P, Levesque M, Elias D *et al.* Preoperative assessment of resectability of hepatic metastases from colonic carcinoma: CT portography vs sonography and dynamic CT. AJR Am J Roentgenol 1992;159:741–4.
14. Matsui O, Kadoya M, Suzuki M *et al.* Work in progress: dynamic sequential computed tomography during arterial portography in the detection of hepatic neoplasms. Radiology 1983;146:721–7.
15. Sherman M, Klein A. AASLD single-topic research conference on hepatocellular carcinoma: conference proceedings. Hepatology 2004;40:1465–73.
16. Tateishi R, Shiina S, Ohki T *et al.* Treatment strategy for hepatocellular carcinoma: expanding the indications for radiofrequency ablation. J Gastroenterol 2009;44 (Suppl 19): 142–6.
17. Ebara M, Ohto M, Sugiura N *et al.* Percutaneous ethanol injection for the treatment of small hepatocellular carcinoma. Study of 95 patients. J Gastroenterol Hepatol 1990;5:616–26.
18. Livraghi T, Giorgio A, Marin G *et al.* Hepatocellular carcinoma and cirrhosis in 746 patients: long-term results of percutaneous ethanol injection. Radiology 1995;197:101–8.
19. Shiina S, Tagawa K, Niwa Y *et al.* Percutaneous ethanol injection therapy for hepatocellular carcinoma: results in 146 patients. AJR Am J Roentgenol 1993;160:1023–8.
20. Seki T, Wakabayashi M, Nakagawa T *et al.* Percutaneous microwave coagulation therapy for patients with small hepatocellular carcinoma: comparison with percutaneous ethanol injection therapy. Cancer 1999;85:1694–702.
21. Rossi S, Di Stasi M, Buscarini E *et al.* Percutaneous RF interstitial thermal ablation in the treatment of hepatic cancer. AJR Am J Roentgenol 1996;167:759–68.
22. Allgaier HP, Deibert P, Zuber I *et al.* Percutaneous radiofrequency interstitial thermal ablation of small hepatocellular carcinoma. Lancet 1999;353:1676–7.
23. Livraghi T, Goldberg SN, Lazzaroni S *et al.* Small hepatocellular carcinoma: treatment with radio-frequency ablation versus ethanol injection. Radiology 1999;210:655–61.
24. Curley SA, Izzo F, Ellis LM *et al.* Radiofrequency ablation of hepatocellular cancer in 110 patients with cirrhosis. Ann Surg 2000;232:381–91.
25. Shiina S, Tateishi R, Arano T *et al.* Radiofrequency ablation for hepatocellular carcinoma: 10-year outcome and prognostic factors. Am J Gastroenterol 2012;107:569–77; quiz 578.
26. Jang HJ, Lim JH, Lee SJ *et al.* Hepatocellular carcinoma: are combined CT during arterial portography and CT hepatic arteriography in addition to

triple-phase helical CT all necessary for preoperative evaluation? Radiology 2000;215:373–80.
27. Rennie D. CONSORT revised--improving the reporting of randomized trials. JAMA 2001;285:2006–7.
28. Efron B. Forcing a sequential experiment to be balanced. Biometrika 1971;58:403.
29. Kitao A, Zen Y, Matsui O et al. Hepatocarcinogenesis: multistep changes of drainage vessels at CT during arterial portography and hepatic arteriography--radiologic-pathologic correlation. Radiology 2009;252:605–14.
30. Tateishi R, Shiina S, Teratani T et al. Percutaneous radiofrequency ablation for hepatocellular carcinoma. An analysis of 1000 cases. Cancer 2005;103:1201–9.
31. Goldberg SN, Grassi CJ, Cardella JF et al. Image-guided tumor ablation: standardization of terminology and reporting criteria. J Vasc Interv Radiol 2009;20:S377–90.
32. Sacks D, McClenny TE, Cardella JF et al. Society of Interventional Radiology clinical practice guidelines. J Vasc Interv Radiol 2003;14:S199–202.
33. Ohki T, Tateishi R, Akahane M et al. Characteristics of hepatocellular carcinoma nodules newly detected by computed tomography during arteriography and arterial portography: preliminary report of a randomized controlled trial. Hepatol Int 2011 (e-pub ahead of print).
34. Minami Y, Kudo M. Review of dynamic contrast-enhanced ultrasound guidance in ablation therapy for hepatocellular carcinoma. World J Gastroenterol 2011;17:4952–9.
35. Numata K, Fukuda H, Morimoto M et al. Use of fusion imaging combining contrast-enhanced ultrasonography with a perflubutane-based contrast agent and contrast-enhanced computed tomography for the evaluation of percutaneous radiofrequency ablation of hypervascular hepatocellular carcinoma. Eur J Radiol 2012;81:2746–53.
36. Masuzaki R, Shiina S, Tateishi R et al. Utility of contrast-enhanced ultrasonography with Sonazoid in radiofrequency ablation for hepatocellular carcinoma. J Gastroenterol Hepatol 2011;26:759–64.
37. Ichikawa T, Saito K, Yoshioka N et al. Detection and characterization of focal liver lesions: a Japanese phase III, multicenter comparison between gadoxetic acid disodium-enhanced magnetic resonance imaging and contrast-enhanced computed tomography predominantly in patients with hepatocellular carcinoma and chronic liver disease. Invest Radiol 2010;45:133–41.
38. Hatanaka K, Kudo M, Minami Y et al. Differential diagnosis of hepatic tumors: value of contrast-enhanced harmonic sonography using the newly developed contrast agent, Sonazoid. Intervirology 2008; 51 (Suppl 1): 61–9.

146

Induction of p53-Dependent p21 Limits Proliferative Activity of Rat Hepatocytes in the Presence of Hepatocyte Growth Factor

Yukiko Inoue[1], Tomoaki Tomiya[1]*, Takako Nishikawa[1], Natsuko Ohtomo[1], Yasushi Tanoue[1], Hitoshi Ikeda[2], Kazuhiko Koike[1]

1 Department of Gastroenterology, Graduate School of Medicine, The University of Tokyo, Tokyo, Japan, 2 Department of Clinical Laboratory Medicine, Graduate School of Medicine, The University of Tokyo, Tokyo, Japan

Abstract

Background: Hepatocyte growth factor (HGF), a potent mitogen for hepatocytes, enhances hepatocyte function without stimulating proliferation, depending on the physiological conditions. p53, a transcription factor, suppresses the cell proliferation by expressing $p21^{WAF1/CIP1}$ in various tissues.

Aim: To investigate the mechanism through which the hepatocytes maintain mitotically quiescent even in the presence of HGF.

Methods: We studied the relationship between p53 and p21 expression and the effect of p53-p21 axis on hepatocyte proliferation in primary cultured rat hepatocytes stimulated by HGF. Hepatic p21 levels are determined serially after partial hepatectomy or sham operation in rats.

Results: DNA synthesis was markedly increased by HGF addition in rat hepatocytes cultured at low density but not at high density. Cellular p53 levels increased in the hepatocytes cultured at both the densities. p21 levels were increased and correlated with cellular p53 levels in hepatocytes cultured at high density but not at low density. When the activity of p53 was suppressed by a chemical inhibitor for p53, cellular p21 levels were reduced, and DNA synthesis was increased. Similarly, p21 antisense oligonucleotide increased the DNA synthesis. In rats after partial hepatectomy, transient elevation of hepatic p21 levels was observed. In contrast, in sham-operated rats, hepatic p21 levels were increased on sustained time scales.

Conclusion: p53-related induction of p21 may suppress hepatocyte proliferation in the presence of HGF in the setting that mitogenic activity of HGF is not elicitable.

Introduction

Proliferation of hepatocytes occurs following the loss of parenchymal cells, while hepatocytes are usually mitotically quiescent. Hepatocyte growth factor (HGF), originally identified as a potent mitogen for hepatocytes in culture, has a pluripotent effect on various types of cells [1–6]. Previous reports indicate that circulating HGF levels in humans are increased with various degrees in physiological and pathological conditions such as acute hepatitis, fulminant hepatic failure, chronic hepatitis, liver cirrhosis, renal failure, post-partial hepatectomy and post-non-hepatectomized abdominal surgery [3,4,7–10]. In the liver of experimental animal models, mitogenic, anti-inflammatory, anti-apoptotic and anti-fibrogenetic activities of HGF have been observed [3,7]. In primary cultured hepatocytes, HGF addition has been shown to facilitate proliferation or function of the cells

depending on the culture condition [2,11]. The mechanism is still under investigation if the specific activities of HGF are selectively expressed. Previously, we reported that HGF exerted mitogenic activity on hepatocytes through the induction of p53, a transcription factor, which increased production of transforming growth factor α (TGF-α), a complete mitogen for hepatocytes [12–14]. However, the mechanism is unknown through which hepatocytes maintain mitotically quiescent when HGF exerts other activities.

Though recent several reports including ours indicate that p53 can stimulate cell proliferation by the specific induction of promoters for growth-associated factors such as TGF-α, p53 is generally recognized as a 'tumor suppressor gene', because, in some pathophysiological conditions, it up-regulates p21, which arrests cell cycle at G1 phase, and inhibits cell proliferation both in vitro and in vivo [14–17]. While p21 expression can be induced by growth-inhibitory stimuli such as DNA damage [18–22], recent

reports indicate the possibility that addition of some growth factors induces p21, and suppresses DNA synthesis especially in malignant cell lines[18,23–28]. However, relationship between p53 and p21 and its significance in non-malignant cells including hepatocytes in the presence of growth factors is still under investigation.

In this paper, we showed that p21 was up-regulated by HGF stimulation through the induction of p53, and suppressed hepatocyte proliferation in the setting that mitogenic activity was not elicitable.

Materials and Methods

Assay for p53 of cultured hepatocytes

Hepatocyte extracts were prepared according to the protocol from the manufacturer of the p53 enzyme-linked immunosorbent assay (ELISA) kit (Roche Molecular Biochemicals, Germany) [14].

Preparation of liver and cultured hepatocytes for p21 assay

Liver tissues and cultured hepatocytes were homogenized in the low salt resuspension buffer (pH 7.4, 50 mmol/L tris (hydroxymethyl) aminomethane, 5 mmol/L ethylenediaminetetraacetic acid, 0.2 mmol/L phenylmethylsulfonyl fluoride 1 μg/mL pepstatin and 0.5 μg/mL leupeptin). The suspensions were incubated with p21 antigen extraction agent (1.0 M potassium chloride, 6% zwittergent (Calbiochem, CA)), and centrifuged. The resultant supernatants were applied to ELISA described below.

Assay for p21 in liver extracts and cultured hepatocytes

The sandwich ELISA for p21 was developed using polyclonal anti p21 IgG (Santa Cruz, CA) and monoclonal p21 antibody (Santa Cruz, CA) as capture and detector antibodies, respectively. Horseradish peroxidase conjugated goat anti-mouse IgG (Zymed, CA) was used to detect the antibody-p21 complex.

The standard curve for p21 (1–164, full length amino acids, Santa Cruz Biotechnology, CA) of this assay made with the buffer showed the lower limit at 1.25 ng/mL. When the sample of rat liver prepared for p21 assay was diluted with the buffer, the dilution curve was similar to the standard curve. When p21 protein was diluted with sample of rat liver or hepatocytes prepared for p21 assay, the dilution curve was similar to the standard curve.

Determination of 5-bromo-2'-deoxy-uridine (BrdU) incorporation and total protein content of cultured hepatocytes

Incorporated BrdU was determined by ELISA, using BrdU labeling and the detection kit III (Roche Molecular Biochemicals, Germany). The total cellular protein was measured by Bradford's method [29].

Experiments with cultured hepatocytes

Hepatocytes were isolated from rat livers according to Seglen's method [30]. The isolated cells were cultured at densities of either 1.2×10^5 cells/cm^2 (high density culture) or 2.5×10^4 cells/cm^2 (low density culture) in the medium and incubated for 27 hours as we previously reported [14]. The medium was changed to Williams' medium E (WE) containing 10% fetal calf serum (FCS), various concentrations of HGF and 0.1 mmol/L BrdU. The cells were harvested serially for the determination of both the cellular p53 and p21 levels and, the BrdU incorporation into cellular DNA.

To study the effect of inhibition of p53 function on p21 levels and DNA synthesis in hepatocytes, the hepatocytes were cultured in WE containing 10% FCS, with or without 10 ng/mL HGF, 1 mmol/L BrdU and various concentrations of pifithrin-α (Alexis Biochemicals, CA) dissolved in dimethyl sulfoxide (DMSO) or the same concentrations of DMSO [31]. The cells were harvested 18 hours later to determine the cellular p21 levels and 24 hours later to determine the BrdU incorporation into cellular DNA.

To examine the effect of inhibition of p21 production on hepatocyte DNA synthesis, the hepatocytes were cultured in WE containing 10% FCS, 10 ng/mL HGF, 1 mmol/L BrdU and various concentrations of either p21 antisense oligonucleotide (5'-GACATCACCAGGATCGGACAT-3'), complementary to position 85–105 of rat p21 mRNA, or nonsense oligonucleotide (5'-GCAACGCTACTACGCAAGTAG-3'), containing the same numbers of G, C, A, and T as the p21 antisense oligonucleotide [32]. The cells were harvested as above, to determine the cellular p21 levels and the BrdU incorporation into cellular DNA.

Animal experiments

Five to six-weeks-old Male Sprague-Dawley rats (Japan SLC, Japan) were subjected to either of two-thirds partial hepatectomy (PH) or sham operation under diethyl ether anesthesia. In sham-operated rats, the abdomen was cut open under similar anesthesia, and the liver was briefly exposed outside the peritoneal cavity. The rats were serially anesthetized with diethyl ether. The liver was perfused through the portal vein with saline. After a near total exsanguination, the liver was excised and used for the p21 assays.

All animal study protocols conformed to and approved by the guideline of the Faculty of Medicine, University of Tokyo for humane care.

Statistical analyses

The differences between two unpaired samples were defined as significant when the p-values by both the Student's t-test and the Mann-Whitney U test were less than 0.05. The dose related effects were tested by one-way analysis of variance followed by Spearman's correlation test.

Results

Changes in DNA synthesis of cultured rat hepatocytes after HGF treatment

We determined the effect of cell density on DNA synthesis of cultured hepatocytes stimulated by HGF. The addition of 10 ng/mL HGF to the medium caused only minor increase on DNA synthesis in hepatocytes cultured at high density. In hepatocytes cultured at low density, DNA synthesis increased after 12 hours of incubation, peaked at 24–30 hours and decreased thereafter by HGF addition (Figure 1). DNA synthesis was not induced significantly in high density cultured hepatocytes by HGF treatment.

Cellular p53 and p21 levels in cultured rat hepatocytes treated with HGF

To investigate the effect of HGF on p53 and p21 expressions and their relationship in proliferating and non-proliferating rat hepatocytes, we determined p53 and p21 protein levels in cultured hepatocytes at low and high density in the presence of various concentration of HGF.

As shown in Figure 2, when rat hepatocytes were cultured at high density with HGF, p53 levels increased at 10 ng/mL or 20 ng/mL of HGF addition (F = 32.5, p<0.01; r = 0.84, p<0.01).

The levels of p53 in high density cultured hepatocytes treated with 10 ng/mL HGF increased after 6 hours and reached a maximum at 24 hours (data not shown), while, in low density cultured hepatocytes treated with 10 ng/mL HGF, p53 levels significantly increased from 6 hours and peaked at 18 to 24 hours of incubation, similar to our previous report [14].

The levels of p21 protein in high density cultured hepatocytes treated with 10 ng/mL HGF increased in a time dependent manner (Figure 3). When hepatocytes cultured at high density were treated with HGF at increasing concentrations, p21 levels at 18 hours after HGF addition increased in a dose-related manner ($F = 73.0$, $p < 0.01$; $r = 0.88$, $p < 0.01$), and correlated with the cellular p53 levels ($r = 0.69$; $p < 0.01$) (Figure 4 and 5A). p21 levels in low density cultured hepatocytes were not increased by HGF addition, nor correlated with p53 levels (Figure 3, 4 and 5B).

p21 levels were increased in a dose related manner by HGF and correlated with p53 levels at high density cultured hepatocytes, while, at low density cultured hepatocytes, p53, but not p21, levels were increased by HGF and there was no correlation between p53 and p21 levels.
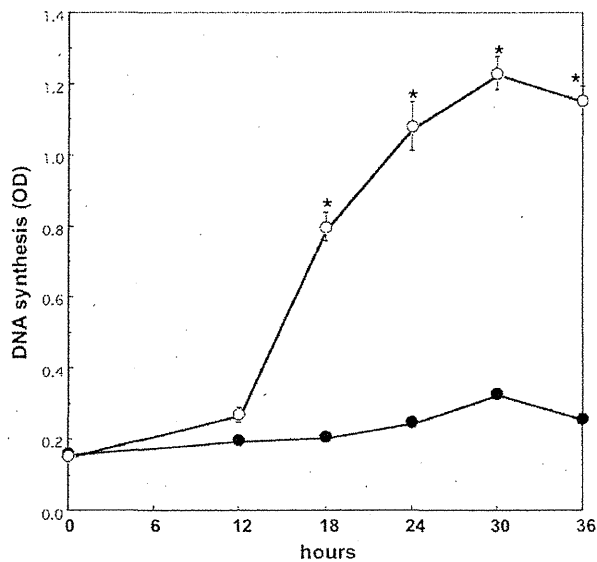

Figure 1. Changes in DNA synthesis of hepatocytes after HGF treatment. Rat hepatocytes were cultured in WE containing 10% FCS, 10 ng/mL HGF and 0.1 mmol/L BrdU, and were harvested serially. Closed circles denote hepatocytes cultured at high density. Open circles denote hepatocytes cultured at low density. Data are mean ± SEM of eight dishes. *p<0.01 compared with the values cultured for 0 hours.
doi:10.1371/journal.pone.0078346.g001

In hepatocytes cultured at low density, HGF addition also increased cellular p53 levels significantly in a dose-related manner up to 10 ng/mL of HGF ($F = 23.4$, $p < 0.01$; $r = 0.90$, $p < 0.01$) (Figure 2).

The effect of pifithrin-α on p21 levels and BrdU incorporation in rat hepatocytes cultured at high and low density in the presence or absence of HGF

To elucidate the relationship between p53 expression and p21 expression as well as DNA synthesis in hepatocytes at non-proliferating condition even in the presence of HGF, we determined the effect of pifithrin-α, a chemical inhibitor of p53, on p21 levels and BrdU incorporation of hepatocytes cultured at high density in the presence of HGF.

The levels of p21 treated with 10 ng/mL HGF for 18 hours in hepatocytes at high density were reduced by the addition of
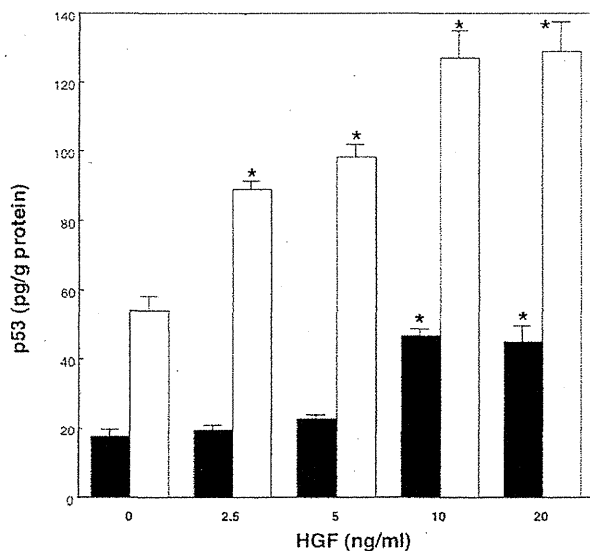

Figure 2. Cellular p53 levels in hepatocytes treated with HGF. Rat hepatocytes were cultured in WE containing 10% FCS and various concentration of HGF for 18 hours. Closed bars denote hepatocytes cultured at high density. Open bars denote hepatocytes cultured at low density. Data are mean ± SEM of four dishes. *p<0.01 compared with the values in the absence of HGF.
doi:10.1371/journal.pone.0078346.g002

Figure 3. Serial changes in p21 protein levels of hepatocytes treated with HGF. Rat hepatocytes were cultured at high density in WE containing 10% FCS and 10 ng/mL HGF, and were harvested serially. Closed circles denote hepatocytes cultured at high density. Open circles denote hepatocytes cultured at low density. Data are mean ± SEM of four dishes. *p<0.01 compared with the values cultured for 0 hours.
doi:10.1371/journal.pone.0078346.g003

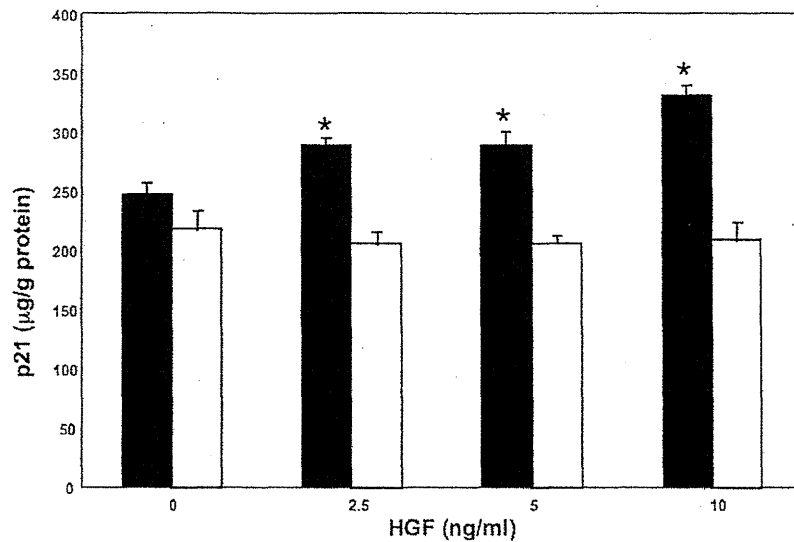**Figure 4. Cellular p21 levels in hepatocytes treated with HGF.** Rat hepatocytes were cultured in WE containing 10% FCS and various concentration of HGF for 18 hours. Closed bars denote hepatocytes cultured at high density. Open bars denote hepatocytes cultured at low density. Data are mean + SEM of four dishes. *p<0.05 compared with the values in the absence of HGF.
doi:10.1371/journal.pone.0078346.g004

pifithrin-α, a chemical inhibitor of p53, when compared with the addition of vehicles (p<0.01) (Figure 6).

In contrast, the levels of p21 in hepatocytes at high density treated without HGF for 18 hours, the values of p21 protein were 211.5±24.9 μg/g protein (mean±standard error), and did not show any significant changes by the addition of pifithrin-α when compared with the addition of vehicles (202.2±57.4 μg/g protein). In addition, the levels of p21 in hepatocytes cultured at low density treated with 10 ng/mL HGF for 18 hours were not affected by pifithrin-α treatment (121.7±18.1 μg/g protein vs137.6±21.8 μg/g protein).
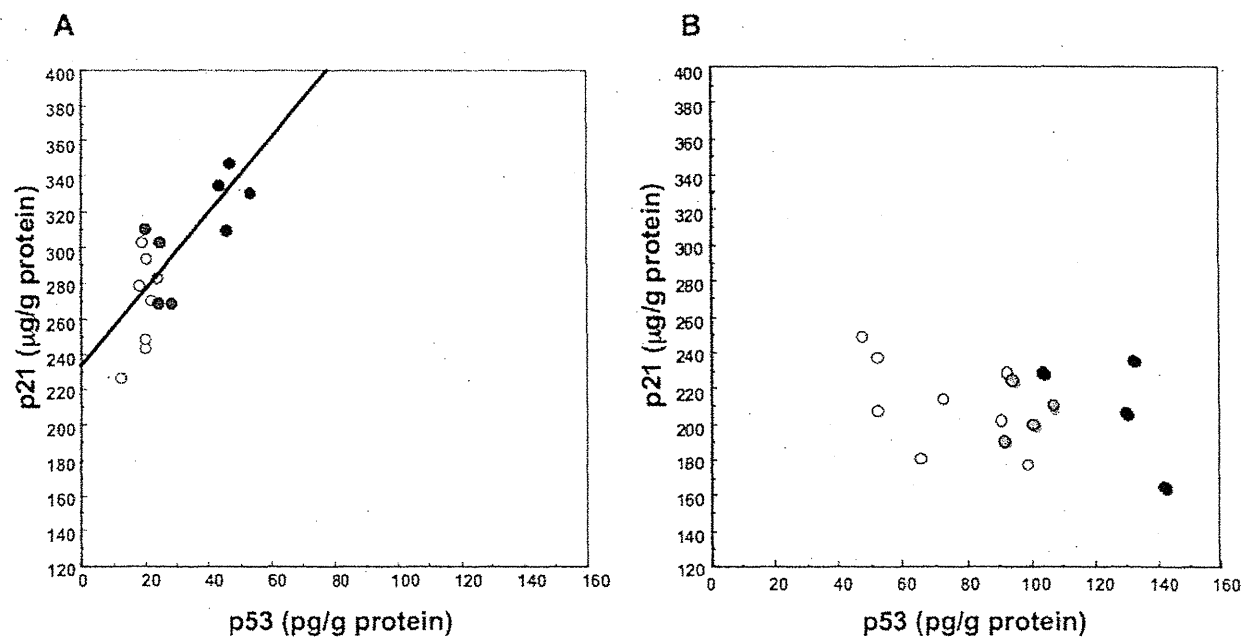
Figure 5. Cellular p53 and p21 levels in hepatocytes treated with HGF. Rat hepatocytes were cultured in WE containing 10% FCS and various concentrations of HGF for 18 hours. Open circles denote hepatocytes cultured in the absence of HGF. Dotted open circles denote hepatocytes cultured with 2.5 ng/mL HGF. Dotted closed circles denote hepatocytes cultured with 5 ng/mL HGF. Closed circles denote hepatocytes cultured with 10 ng/mL HGF. (A) Hepatocytes cultured at high density. (B) Hepatocytes cultured at low density.
doi:10.1371/journal.pone.0078346.g005
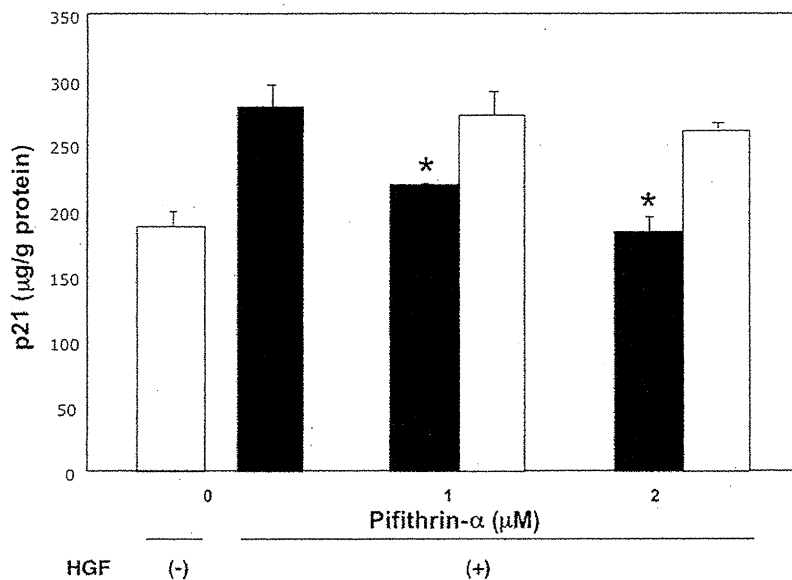
Figure 6. The effect of pifithrin-α on p21 levels of hepatocytes in the presence of HGF. Rat hepatocytes were cultured at high density in WE containing 10% FCS, 10 ng/mL HGF, along with various concentrations of pifithrin-α, the chemical inhibitor of p53, dissolved in DMSO, or DMSO of the same concentration for 18 hours. An open bar denotes hepatocytes cultured in the absence of HGF. Closed bars denote hepatocytes cultured with pifithrin-α in the presence of 10 ng/mL HGF. Dotted bars denote hepatocytes cultured with DMSO in the presence of 10 ng/mL HGF. Data are mean ± SEM of four dishes. *$p<0.05$ compared with the values treated only with HGF or values treated with HGF and DMSO.
doi:10.1371/journal.pone.0078346.g006

The levels of BrdU incorporation treated with 10 ng/mL of HGF for 24 hours were increased significantly by the addition of 2 μM of pifithrin-α, when compared with the addition of vehicles ($p<0.01$) (Figure 7). The total cellular protein levels were not affected by the addition of either pifithrin-α or vehicles (data not shown).

p21 levels were reduced and DNA synthesis was significantly increased by pifithrin-α a chemical inhibitor of p53, in the presence of HGF in high density cultured hepatocytes.

The effect of p21 antisense oligonucleotides on BrdU incorporation in rat hepatocytes cultured at high density in the presence of HGF

We investigated the effect of suppression of p21 expression on DNA synthesis in non-proliferationg hepatocytes in the presence of HGF. BrdU incorporation in hepatocytes cultured at high density in the presence of 10 ng/mL of HGF was significantly increased after a 24-hour exposure to p21 antisense oligonucleotide, when compared with that of hepatocytes treated with the nonsense oligonucleotide ($p<0.01$) (Figure 8). The total cellular protein levels were not affected by the addition of either oligonucleotide (data not shown). Suppression of p21 expression increased the DNA synthesis in the presence of HGF in high density cultured hepatocytes.

p21 levels in the liver after two-thirds PH or sham operation in rats

To study p21 expression profile in regenerating and quiescent rat liver, we determined hepatic p21 levels in rats after PH and sham operation. Hepatic p21 levels were increased to the maximal levels at 4 hours, and decreased to the basal levels at 8 hours after PH with minor increase at 48 hours. In contrast, hepatic p21 levels of sham-operated rats were increased up to 2.5-fold higher than preoperative levels at 12 to 48 hours and decreased to the

Figure 7. The effect of pifithrin-α on DNA synthesis of hepatocytes in the presence of HGF. Rat hepatocytes were cultured at high density in the same medium as described in the legend of Figure 6, except that the medium contained 1 mmol/L BrdU, for 24 hours. An open bar denotes hepatocytes cultured in the absence of HGF. Closed bars denote hepatocytes cultured with pifithrin-α in the presence of 10 ng/mL HGF. A dotted bar denotes hepatocytes cultured with DMSO in the presence of 10 ng/mL HGF. Data are mean ± SEM of eight dishes. *$p<0.01$ compared with the values treated only with HGF or values treated with HGF and DMSO.
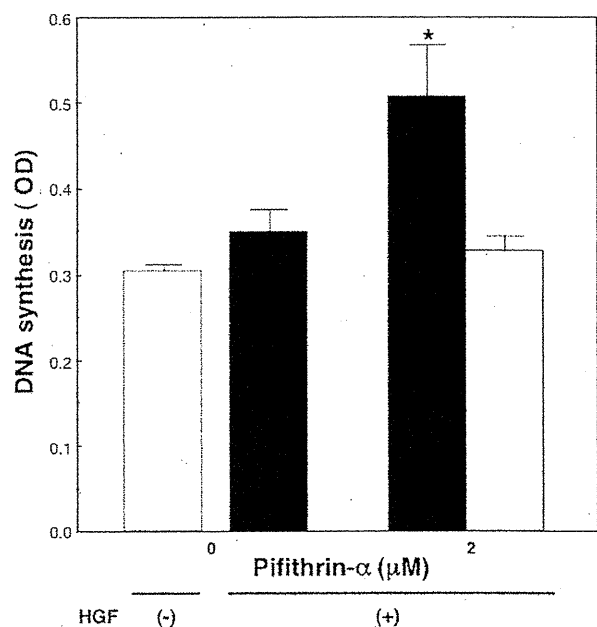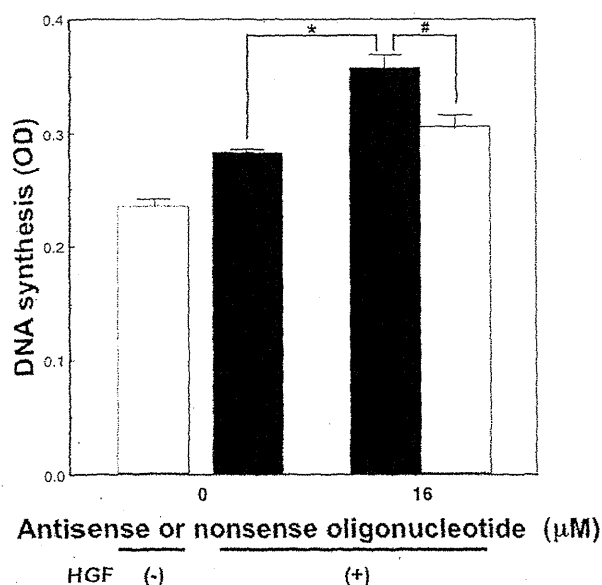doi:10.1371/journal.pone.0078346.g007

Figure 8. The effect of p21 antisense on DNA synthesis of hepatocytes in the presence of HGF. Rat hepatocytes were cultured at high density in WE containing 10% FCS, 10 ng/mL HGF, 1 mmol/L BrdU, along with various concentrations of either p21 antisense or nonsense oligonucleotide for 24 hours. An open bar denotes hepatocytes cultured in the absence of HGF. Closed bars denote hepatocytes cultured with p21 antisense oligonucleotide in the presence of 10 ng/mL HGF. A dotted bar denotes hepatocytes cultured with nonsense oligonucleotide in the presence of 10 ng/mL HGF. Data are mean ± SEM of eight dishes. *p<0.05 compared with the values treated only with HGF, and #p<0.01 compared with the values treated with HGF and nonsense oligonucleotide.
doi:10.1371/journal.pone.0078346.g008

Figure 9. Changes in hepatic p21 levels after two thirds partial hepatectomy in rats. Data are mean ± SEM of four rats. Open and closed circles indicate the hepatic p21 levels in partially hepatectomized rats and in sham-operated rats, respectively. *p<0.05 compared with the values at 0 hour, and #p<0.05 compared with the values of partially hepatectomized rats.
doi:10.1371/journal.pone.0078346.g009

preoperative level at 72 hours. Hepatic p21 levels were significantly higher in sham-operated rats than in rats after PH except within 4 hours after surgery (Figure 9). In sham-operated rats, hepatic p21 levels were increased on sustained time scales while only transient elevation was observed in partial hepatectomized rats.

Discussion

We confirmed that DNA synthesis was not induced significantly in hepatocytes cultured at high density even in the presence of HGF, as we previously reported [2]. HGF seems to increase p53 and p21, and maintain mitotically quiescent in the hepatocytes.

We determined p21 protein levels in vitro and in vivo using newly developed ELISA system. Although p21 expression has been extensively studied in proliferating and non-proliferating hepatocytes and in the liver with or without regenerative stimuli [33–36], the results are inconsistent. In most of these reports, p21 mRNA levels were studied, or p21 protein levels were determined by Western blotting. When p21 synthesis is induced, p21 mRNA levels are generally up-regulated. Furthermore, p21 synthesis is further increased at the post-transcriptional level in hepatocytes [37]. Thus, in this study, we determined p21 protein expressions which may function as transcription factor. In addition, to avoid the unstable results, we determined p21 protein levels utilizing a quantitative method which was sensitive enough to detect p21 during observation periods in vitro and in vivo.
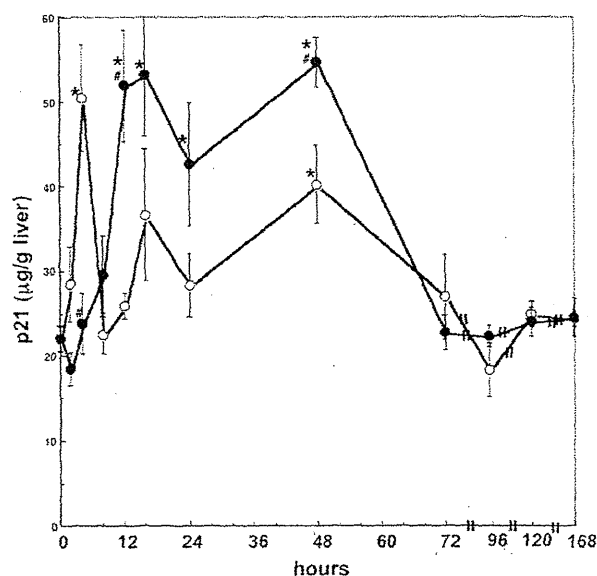
We suppressed p53 activity and p21 expression using pifithrin-α and a p21 antisense oligonucleotide, respectively. Pifithrin-α disturbs the nuclear transport of p53 leading to the inhibition of the function of p53 in vitro and in vivo [31,38]. We used pifithrin-α at the same concentration as previously reported in hepatocytes [14,38]. The efficacy of the p21 antisense oligonucleotide was also previously reported in other cell culture systems [32].

Previously, we reported that the addition of HGF to the medium increased p53 contents in hepatocytes cultured at low density followed by the increase of DNA synthesis by hepatocytes [14]. In this present paper, we showed that the p53 levels were also increased by HGF treatment in hepatocytes cultured at high density which did not show apparent burst of DNA synthesis. The mechanisms responsible for the increase of p53 in hepatocytes by HGF are still undefined. However, it has been reported that activation of mitogen activated protein (MAP) kinase influences transcription factors including p53 [39]. Considering that MAP kinase is thought to mediate the intracellular effects of HGF [40], HGF might increase p53 through the interaction of MAP kinase and p53. Recently, the relationship between growth factors and p53 has been shown in a couple of reports. HGF was shown to increase p53 expression in a rat epithelial cell line, and insulin-like growth factor I was reported to induce p53 expression in cardiac muscle cells [41,42]. In primary cultured rat hepatocytes, epidermal growth factor (EGF) was shown to induce p53 expression in a phosphatidylinositol-3 kinase-dependent way [36]. In addition, p53 null hepatocytes were reported to be refractory to the stimulation of EGF [43].

p21 is known to be induced by p53-dependent and -independent mechanisms according to the cell types and situations [18]. Following DNA damage, p53 appears to be necessary for p21 induction in various kinds of cell types [18]. Many experiments showed that p21 was the major effector of p53 in inducing growth arrest in malignant cells [17,18]. Furthermore,

p21 was reported to be induced by p53 and negatively regulate cell proliferation in normal fibroblasts without DNA damage [44]. In addition, expression of the p53-induced p21 was greatly diminished by targeting p53 with anti-p53 antibody, and the cells reentered S-phase in fibroblasts [45]. We showed that cellular levels of p21 correlated with those of p53 and suppression of p53 activity by pifithrin-α resulted in the decrease of p21 levels followed by an increase of DNA synthesis in hepatocytes cultured at high density. p21 seems to be induced by p53 dependent mechanism in the present culture system of hepatocytes leading to suppression of proliferation.

Previous several reports have shown that growth factors can induce p21 production and suppress cell proliferation. Transient induction of p21 mRNA following stimulation of growth factors such as EGF, platelet-derived growth factor and fibroblast growth factor is reported in several cell lines, leading to cell cycle arrest [18,26–28,46]. p21 was up-regulated by HGF addition, and mediated growth inhibition in a hepatoma cell-line [23–25]. In primary cultured rat and mouse hepatocytes, p21 is reported to be induced by EGF and to have a role in the blockage of hepatocyte replication of the second round but not of the first round [33]. In addition, Wierod et.al reported that EGF induced p21 through the activation of p53 in primary cultured rat hepatocytes [36]. However, they noted that EGF-induced p21 might positively regulate DNA synthesis, since stimulatory effect of EGF on DNA synthesis was abrogated when p53 was inhibited, and rescued by ectopical p21 addition [36]. It was reported that the role of p21 might differ by its concentrations [47]. To examine the role of intrinsic p21 in regulating DNA synthesis of hepatocytes, the effect of p21 inhibition in the presence of EGF should be studied. In our culture system using primary cultured rat hepatocytes and HGF, we showed that suppression of HGF-induced increase of p21 production positively regulated DNA synthesis by hepatocytes cultured at high density, suggesting that up-regulation of p21 maintained mitotically quiescent in hepatocytes in the presence of HGF. No apparent change of p21 expression was caused by pifithrin-α in hepatocytes cultured without HGF treatment, suggesting the effect of p53 inhibition on baseline p21 seemed to be minimal. In the high density cultured hepatocytes, protein production such as albumin is increased by HGF addition [2,11]. In contrast, in hepatocytes cultured at low density, we previously reported that HGF induced TGF-α production through the induction of p53, and hepatocyte proliferation occurred [14]. It is possible to speculate that induction of diverse effector genes of p53 plays a role in the expression of different activities of HGF. Further investigations would be required to clarify the mechanism(s) of the selective expression of p53 related genes in hepatocytes in different conditions stimulated by HGF.

Previous experiments in rats showed that hepatic levels of p21 protein after PH determined by Western blot analysis were increased at two time points, first immediately after resection and second after the peak of DNA synthesis. In sham operated rats, the p21 levels were almost undetectable throughout the 7-day time course [34]. Controversially, some reports demonstrated that hepatic p21 protein levels determined by Western blot analysis were decreased in partially hepatectomized rats and increased in sham-operated rats. The maximum decrease was observed immediately before the peak DNA synthesis, with increased p53 levels after PH, while the levels began to increase immediately after sham operation, and continued up to 48 hours of observation [48]. In mice after PH, p21 expression was reported to be increased before DNA synthesis of hepatocytes and reached maximum after the peak of hepatocyte DNA synthesis on Western blot analysis [49]. In the present study, hepatic p21 protein levels were increased immediately after PH, but returned to preoperative levels within 8 hours, while a sustained increase of p21 levels was observed after sham operation up to 48 hours. The reason for the discrepancy of the data is unclear. The difference of the assay system might influence the observations. Previously, we reported that hepatic p53 levels as well as hepatic and circulating HGF levels were increased after sham operation without the increase of hepatocyte proliferation [12,14], while, in rats after PH, hepatic p53 levels were increased and reached maximal levels, when hepatic HGF levels have been shown to reach maximum prior to an increase in hepatocyte proliferation [13,14]. These observations raise the possibility that the increase of p21 is related to keep quiescent when hepatocyte proliferation is not physiologically required even though HGF levels are increased. Previous studies described that c-Jun controlled hepatocyte proliferation by a p53/p21-dependent mechanism in mice [50]. p21 knock out mice demonstrated markedly accelerated hepatocyte proliferation compared to cogenic wild-type mice after PH [49]. These reports support our hypothesis. Significance of the transient increase of hepatic p21 levels after PH is still to be elucidated. The role of p21 may change depending on its concentration; p21 promotes cyclin/cdk complex assembly at low concentration, whereas, at higher concentrations, p21 is inhibitory to cdk in human normal fibroblast and human osteosarcoma cell [47]. The levels and the timing of the increase might influence the activity of p21.

Author Contributions

Conceived and designed the experiments: YI TT. Performed the experiments: YI TT TN YT. Analyzed the data: YI TT NO. Contributed reagents/materials/analysis tools: TT KK. Wrote the paper: YI TT HI.

References

1. Michalopoulos GK (2009) Liver regeneration after partial hepatectomy: critical analysis of mechanistic dilemmas. Am J Pathol 176: 2–13.
2. Yamaoka M, Hirata K, Ogata I, Tomiya T, Nagoshi S, et al. (1998) Enhancement of albumin production by hepatocyte growth factor in rat hepatocytes: distinction in mode of action from stimulation of DNA synthesis. Liver 18: 52–59.
3. Zarnegar R, Michalopoulos GK (1995) The many faces of hepatocyte growth factor: from hepatopoiesis to hematopoiesis. J Cell Biol 129: 1177–1180.
4. Fausto N, Campbell JS, Riehle KJ (2006) Liver regeneration. Hepatology 43: S45–53.
5. Tomiya T, Inoue Y, Yanase M, Arai M, Ikeda H, et al. (2004) Treatment with leucine stimulates the production of hepatocyte growth factor in vivo. Biochem Biophys Res Commun 322: 772–777.
6. Fujiwara K, Nagoshi S, Ohno A, Hirata K, Ohta Y, et al. (1993) Stimulation of liver growth by exogenous human hepatocyte growth factor in normal and partially hepatectomized rats. Hepatology 18: 1443–1449.
7. Mizuno S, Nakamura T (2007) Hepatocyte growth factor: a regenerative drug for acute hepatitis and liver cirrhosis. Regen Med 2: 161–170.
8. Tomiya T, Nagoshi S, Fujiwara K (1996) Blood hepatocyte growth factor levels in chronic renal failure patients. Nephron 73: 735.
9. Tomiya T, Nagoshi S, Fujiwara K (1992) Significance of serum human hepatocyte growth factor levels in patients with hepatic failure. Hepatology 15: 1–4.
10. Tomiya T, Tani M, Yamada S, Hayashi S, Umeda N, et al. (1992) Serum hepatocyte growth factor levels in hepatectomized and nonhepatectomized surgical patients. Gastroenterology 103: 1621–1624.
11. Takehara T, Matsumoto K, Nakamura T (1992) Cell density-dependent regulation of albumin synthesis and DNA synthesis in rat hepatocytes by hepatocyte growth factor. J Biochem (Tokyo) 112: 330–334.
12. Tomiya T, Ogata I, Fujiwara K (1998) Transforming growth factor alpha levels in liver and blood correlate better than hepatocyte growth factor with hepatocyte proliferation during liver regeneration. Am J Pathol 153: 955–961.
13. Tomiya T, Ogata I, Yamaoka M, Yanase M, Inoue Y, et al. (2000) The mitogenic activity of hepatocyte growth factor on rat hepatocytes is dependent upon endogenous transforming growth factor-alpha. Am J Pathol 157: 1693–1701.

14. Inoue Y, Tomiya T, Yanase M, Arai M, Ikeda H, et al. (2002) p53 May positively regulate hepatocyte proliferation in rats. Hepatology 36: 336–344.
15. Shin TH, Paterson AJ, Kudlow JE (1995) p53 stimulates transcription from the human transforming growth factor alpha promoter: a potential growth-stimulatory role for p53. Mol Cell Biol 15: 4694–4701.
16. El-Deiry WS, Tokino T, Velculescu VE, Levy DB, Parsons R, et al. (1993) WAF1, a potential mediator of p53 tumor suppression. Cell 75: 817–825.
17. Vousden KH, Prives C (2009) Blinded by the Light: The Growing Complexity of p53. Cell 137: 413–431.
18. Abbas T, Dutta A (2009) p21 in cancer: intricate networks and multiple activities. Nat Rev Cancer 9: 400–414.
19. Harper JW, Adami GR, Wei N, Keyomarsi K, Elledge SJ (1993) The p21 Cdk-interacting protein Cip1 is a potent inhibitor of G1 cyclin-dependent kinases. Cell 75: 805–816.
20. Noda A, Ning Y, Venable SF, Pereira-Smith OM, Smith JR (1994) Cloning of senescent cell-derived inhibitors of DNA synthesis using an expression screen. Exp Cell Res 211: 90–98.
21. Macleod KF, Sherry N, Hannon G, Beach D, Tokino T, et al. (1995) p53-dependent and independent expression of p21 during cell growth, differentiation, and DNA damage. Genes Dev 9: 935–944.
22. El-Deiry WS, Harper JW, O'connor PM, Velculescu VE, Canman CE, et al. (1994) WAF1/CIP1 is induced in p53-mediated G1 arrest and apoptosis. Cancer Res 54: 1169–1174.
23. Tsukada Y, Tanaka T, Miyazawa K, Kitamura N (2004) Involvement of down-regulation of Cdk2 activity in hepatocyte growth factor-induced cell cycle arrest at G1 in the human hepatocellular carcinoma cell line HepG2. J Biochem 136: 701–709.
24. Shima N, Stolz DB, Miyazaki M, Gohda E, Higashio K, et al. (1998) Possible involvement of p21/waf1 in the growth inhibition of HepG2 cells induced by hepatocyte growth factor. J Cell Physiol 177: 130–136.
25. Han J, Tsukada Y, Hara E, Kitamura N, Tanaka T (2005) Hepatocyte growth factor induces redistribution of p21(CIP1) and p27(KIP1) through ERK-dependent p16(INK4a) up-regulation, leading to cell cycle arrest at G1 in HepG2 hepatoma cells. J Biol Chem 280: 31548–31556.
26. Fan Z, Lu Y, Wu X, Deblasio A, Koff A, et al. (1995) Prolonged induction of p21Cip1/WAF1/CDK2/PCNA complex by epidermal growth factor receptor activation mediates ligand-induced A431 cell growth inhibition. J Cell Biol 131: 235–242.
27. Chin YE, Kitagawa M, Su WC, You ZH, Iwamoto Y, et al. (1996) Cell growth arrest and induction of cyclin-dependent kinase inhibitor p21 WAF1/CIP1 mediated by STAT1. Science 272: 719–722.
28. Gartel AL, Tyner AL (1999) Transcriptional regulation of the p21((WAF1/CIP1)) gene. Exp Cell Res 246: 280–289.
29. Bradford MM (1976) A rapid and sensitive method for the quantitation of microgram quantities of protein utilizing the principle of protein-dye binding. Anal Biochem 72: 248–254.
30. Seglen PO (1976) Preparation of isolated rat liver cells. Methods Cell Biol 13: 29–83.
31. Komarov PG, Komarova EA, Kondratov RV, Christov-Tselkov K, Coon JS, et al. (1999) A chemical inhibitor of p53 that protects mice from the side effects of cancer therapy. Science 285: 1733–1737.
32. Israsena N, Kessler JA (2002) Msx2 and p21(CIP1/WAF1) mediate the proapoptotic effects of bone morphogenetic protein-4 on ventricular zone progenitor cells. J Neurosci Res 69: 803–809.
33. Fremin C, Bessard A, Ezan F, Gailhouste L, Regeard M, et al. (2009) Multiple division cycles and long-term survival of hepatocytes are distinctly regulated by extracellular signal-regulated kinases ERK1 and ERK2. Hepatology 49: 930–939.
34. Albrecht JH, Rieland BM, Nelsen CJ Ahonen CL (1999) Regulation of G(1) cyclin-dependent kinases in the liver: role of nuclear localization and p27 sequestration. Am J Physiol 277: G1207–1216.
35. Albrecht JH, Meyer AH, Hu MY (1997) Regulation of cyclin-dependent kinase inhibitor p21(WAF1/Cip1/Sdi1) gene expression in hepatic regeneration. Hepatology 25: 557–563.
36. Wierod L, Rosseland CM, Lindeman B, Oksvold MP, Grosvik H, et al. (2008) Activation of the p53–p21(Cip1) pathway is required for CDK2 activation and S-phase entry in primary rat hepatocytes. Oncogene 27: 2763–2771.
37. Park JS, Qiao L, Gilfor D, Yang MY, Hylemon PB, et al. (2000) A role for both Ets and C/EBP transcription factors and mRNA stabilization in the MAPK-dependent increase in p21 (Cip-1/WAF1/mda6) protein levels in primary hepatocytes. Mol Biol Cell 11: 2915–2932.
38. Chou WW, Guh JY, Tsai JF, Hwang CC, Chen HC, et al. (2008) Arecoline-induced growth arrest and p21WAF1 expression are dependent on p53 in rat hepatocytes. Toxicology 243: 1–10.
39. Milne DM, Campbell DG, Caudwell FB, Meek DW (1994) Phosphorylation of the tumor suppressor protein p53 by mitogen-activated protein kinases. J Biol Chem 269: 9253–9260.
40. Faletto DL, Kaplan DR, Halverson DO, Rosen EM, Vande Woude GF (1993) Signal transduction in c-met mediated motogenesis. EXS 65: 107–130.
41. Conner EA Wirth PJ, Kiss A, Santoni-Rugiu E, Thorgeirsson SS (1997) Growth inhibition and induction of apoptosis by HGF in transformed rat liver epithelial cells. Biochem Biophys Res Commun 236: 396–401.
42. Chen WH, Pellegata NS, Wang PH (1995) Coordinated effects of insulin-like growth factor I on inhibitory pathways of cell cycle progression in cultured cardiac muscle cells. Endocrinology 136: 5240–5243.
43. Bellamy CO, Clarke AR, Wyllie AH, Harrison DJ (1997) p53 Deficiency in liver reduces local control of survival and proliferation, but does not affect apoptosis after DNA damage. FASEB J 11: 591–599.
44. Atadja P, Wong H, Garkavtsev I, Veillette C, Riabowol K (1995) Increased activity of p53 in senescing fibroblasts. Proc Natl Acad Sci U S A 92: 8348–8352.
45. Gire V, Wynford-Thomas D (1998) Reinitiation of DNA synthesis and cell division in senescent human fibroblasts by microinjection of anti-p53 antibodies. Mol Cell Biol 18: 1611–1621.
46. Michieli P, Chedid M, Lin D, Pierce JH, Mercer WE, et al. (1994) Induction of WAF1/CIP1 by a p53-independent pathway. Cancer Res 54: 3391–3395.
47. Labaer J, Garrett MD, Stevenson LF, Slingerland JM, Sandhu C, et al. (1997) New functional activities for the p21 family of CDK inhibitors. Genes Dev 11: 847–862.
48. Timchenko NA, Harris TE, Wilde M, Bilyeu TA, Burgess-Beusse BL, et al. (1997) CCAAT/enhancer binding protein alpha regulates p21 protein and hepatocyte proliferation in newborn mice. Mol Cell Biol 17: 7353–7361.
49. Albrecht JH, Poon RY, Ahonen CL, Rieland BM, Deng C, et al. (1998) Involvement of p21 and p27 in the regulation of CDK activity and cell cycle progression in the regenerating liver. Oncogene 16: 2141–2150.
50. Stepniak E, Ricci R, Eferl R, Sumara G, Sumara I, et al. (2006) c-Jun/AP-1 controls liver regeneration by repressing p53/p21 and p38 MAPK activity. Genes Dev 20: 2306–2314.

Original Article

Perihepatic lymph node enlargement is a negative predictor for sustained responses to pegylated interferon-α and ribavirin therapy for Japanese patients infected with hepatitis C virus genotype 1

Hiromi Hikita,[1]* Kenichiro Enooku,[1,2]* Yumiko Satoh,[1] Haruhiko Yoshida,[2]
Hayato Nakagawa,[1,2] Ryota Masuzaki,[2] Ryosuke Tateishi,[2] Yoko Soroida,[1] Mamiko Sato,[1]
Atsushi Suzuki,[1] Hiroaki Gotoh,[1] Tomomi Iwai,[1] Hiromitsu Yokota,[1] Kazuhiko Koike,[2]
Yutaka Yatomi[1] and Hitoshi Ikeda[1,2]

Departments of [1]Clinical Laboratory Medicine and [2]Gastroenterology, Graduate School of Medicine, The
University of Tokyo, Tokyo, Japan

Aim: Although perihepatic lymph node enlargement (PLNE) is reportedly associated with the negative outcome of interferon therapy for chronic hepatitis C, there were limitations in that the results were obtained in patients with various genotypes, viral loads and treatment regimens. We aimed to precisely clarify the significance of PLNE in interferon therapy for chronic hepatitis C.

Methods: Between December 2004 and June 2005, 112 patients with hepatitis C virus (HCV) genotype 1 and HCV RNA of more than 100 KIU/mL were enrolled, who underwent pegylated interferon-α plus ribavirin therapy thereafter. PLNE was defined as a perihepatic lymph node of more than 1 cm in the longest axis by ultrasonography.

Results: The sustained virological response (SVR) rate was lower in patients with PLNE (4/22, 18.2%) than in those without (37/90, 41.1%; P = 0.045) and viral load decline was smaller in patients with PLNE than in those without (P = 0.028). The

proportion of PLNE positive patients was the smallest in the SVR group (P = 0.033) among the patient groups divided by the treatment outcome. PLNE was retained as a negative predictor for SVR by multivariate logistic regression analysis (P = 0.012). Furthermore, PLNE was not significantly associated with the mutations at HCV core protein and at interferon sensitivity-determining region, or interleukin-28B polymorphism in 45 patients with HCV genotype 1, enrolled between December 2011 and March 2012.

Conclusion: PLNE is a negative predictor for SVR in patients with HCV genotype 1 and HCV RNA of more than 100 KIU/mL treated with pegylated interferon-α plus ribavirin, independent of other known predictors for SVR.

Key words: chronic hepatitis C, hepatitis C virus core protein, interferon sensitivity-determining region, interleukin-28B

INTRODUCTION

PERIHEPATIC LYMPH NODE enlargement (PLNE) is frequently observed in patients with chronic liver disease,[1] especially in those with hepatitis C.[2,3] Although

it has been shown that PLNE is associated with inflammatory activity, stage of liver fibrosis or hepatitis C viral load,[3–8] the reported findings were inconsistent,[2,9] suggesting that the clinical significance of PLNE has not been fully established yet. We have recently reported that PLNE is a negative predictor for hepatocellular carcinoma (HCC) development in chronic hepatitis C patients.[10]

Regarding PLNE and efficacy of interferon (IFN) therapy for chronic hepatitis C, PLNE was reportedly more frequently found in non-responders.[11,12] Dietrich et al. reported that perihepatic lymph node volume before IFN treatment was significantly larger in non-responders than in sustained virological responders,

based on a study in which the patients had various genotypes and viral loads and were treated with IFN-α with or without ribavirin (RBV).[11] Soresi *et al.* reported that PLNE was more frequent in non-responders to IFN-α with RBV, although this association did not reach statistical significance by logistic regression analysis, in which the patients also had various genotypes.[12] We also reported that the sustained virological response (SVR) rate in patients who received IFN therapy was significantly lower in patients with PLNE than in those without, although our patients also had various genotypes and viral loads, and treatment regimens were various including IFN-α or pegylated IFN-α (PEG IFN) with or without RBV.[10] It is well known that patients with hepatitis C virus (HCV) genotype 1 and high baseline viral load are most difficult to treat with IFN[13] and that PEG IFN plus RBV has been the most effective standard of care for chronic hepatitis C until telaprevir emerged.[14] Thus, the previous results regarding PLNE and efficacy of IFN therapy for chronic hepatitis C had limitations, because they were analyzed with various genotypes, viral loads and treatment regimens.

In this study, in order to precisely clarify the potential association between PLNE and efficacy of IFN therapy for chronic hepatitis C, we analyzed the patients with HCV genotype 1 and HCV RNA of more than 100 KIU/mL at the start of therapy by PEG IFN with RBV in the well-characterized chronic hepatitis C cohort, in which liver stiffness values were found to be a risk for HCC development.[15]

METHODS

Subjects

THE PREVIOUS COHORT in which we originally analyzed the risk of liver stiffness for HCC development was employed; 866 chronic hepatitis C patients were enrolled between December 2004 and June 2005 at the Department of Gastroenterology, The University of Tokyo Hospital.[15] Among these patients, 112 patients, who had HCV genotype 1 and HCV RNA >100 KIU/mL, underwent PEG IFN plus RBV therapy after the enrollment. The potential association between PLNE and efficacy of PEG IFN plus RBV therapy was examined with these patients. When each subject was screened for HCC with ultrasonography at or immediately after the enrollment, the presence of PLNE was evaluated. The criteria to identify PLNE were previously described, and PLNE was defined as a lymph node at perihepatic area which was at least 1 cm in the longest axis.[10]

Moreover, between December 2011 and March 2012, 45 chronic hepatitis C patients with genotype 1 were enrolled at the Department of Gastroenterology, The University of Tokyo Hospital, to assess the potential association between PLNE and the known factors to predict the response to IFN therapy, namely, the mutations at position 70 of HCV core protein, those at IFN sensitivity-determining region (ISDR) of NS5A protein or interleukin (IL)-28B polymorphism.

The present study was carried out in accordance with the ethical guidelines of the Declaration of Helsinki and was approved by the Institutional Research Ethics Committee of the authors' institution. Informed consent was obtained for the use of the samples in this study.

Laboratory tests

Sequences of ISDR and the core region of HCV were determined by direct sequencing after amplification by reverse transcription and polymerase chain reaction as reported previously.[16,17] Genetic polymorphism in one tagging single nucleotide polymorphism located near the *IL-28B* gene (rs8099917) was determined by direct sequencing.[18] Homozygosity (GG) or heterozygosity (TG) of the minor sequence was defined as having the IL-28B minor allele, whereas homozygosity for the major sequence (TT) was defined as having the IL-28B major allele. Null virological response (NVR) was defined as detectable HCV RNA by qualitative polymerase chain reaction with a lower detection limit of 50 IU/mL (Amplicor; Roche Diagnostic Systems, Pleasanton, CA, USA) during the therapy. SVR was defined as undetectable HCV RNA 24 weeks after the completion of therapy. Relapse was defined as reappearance of HCV RNA after the completion of therapy. HCV RNA was quantitated using Amplicore HCV ver. 2.0 (Roche, Tokyo, Japan) or Cobas Ampliprep/Cobas TaqMan assay system (Roche, Tokyo, Japan). HCV genotype was determined based on the serotyping assay (SRL, Tokyo, Japan) or direct sequence analysis.[19]

Statistical analysis

Data were expressed as the mean ± standard deviation (SD) unless otherwise indicated. The categorical variables were compared by χ^2-test or Fischer's exact test, whereas continuous variables were compared by unpaired Student's *t*-test (parametric), Mann–Whitney *U*-test (non-parametric), Kruskal–Wallis rank sum test (non-parametric) or Wilcoxon rank sum test (non-parametric). For comparing group means, we used ANOVA. In the analysis of predicting factors for the responses to PEG IFN plus RBV therapy, the following

156

variables were tested in univariate and multivariate logistic regression analysis: age, sex, serum albumin, aspartate aminotransferase (AST), alanine aminotransferase (ALT), γ-glutamyltransferase (GGT), alkaline phosphatase, total bilirubin, α-fetoprotein (AFP) levels, prothrombin activity (%), liver stiffness values, platelet count, HCV viral load and the presence of PLNE. Factors that had a P-value of less than 0.4 in univariate analysis were subsequently included in multivariate logistic regression analysis. A P-value of less than 0.05 was considered significant. Data processing and analysis were performed using StatView ver. 5.0 (SAS Institute, Cary, NC, USA) and SPSS ver. 14.0 (SPSS, Chicago, IL, USA) software.

RESULTS

Association between PLNE and efficacy of PEG IFN plus RBV therapy

THE CLINICAL FEATURES of patients are summarized according to the presence or absence of PLNE in Table 1. All the patients were infected with HCV genotype 1 and had a high viral load (HCV RNA >100 KIU/mL). No patients were co-infected with hepatitis B virus. PLNE was observed in 22 of 112 (20.0%) patients analyzed.

PEG IFN-2a was administrated in 24 patients, while PEG IFN-2b in 88 patients. This ratio between patients treated with PEG IFN-2a and those with PEG IFN-2b was not different between patients with PLNE and those without (data not shown). Most of the patients were treated when the extended treatment of PEG IFN plus RBV therapy for more than 48 weeks was not generally performed in Japan; 27 of 112 (24.1%) patients received PEG IFN plus RBV for more than 48 weeks up to 72 weeks. After PEG IFN plus RBV therapy, SVR was achieved in 41 of 112 (36.6%) patients in this cohort. Between patients with PLNE and those without, the SVR rate was significantly lower in the former (4/22, 18.2%) than in the latter (37/90, 41.1%) (P = 0.045; Table 1). Of note, liver stiffness values as well as serum albumin levels, prothrombin activity and platelet count, which may be suggestive of liver fibrosis, were not different between patients with PLNE and those without (Table 1). Only serum GGT levels among the blood parameters were significantly lower in patients with PLNE than in those without.

To examine whether PLNE may influence virological response, the viral loads before treatment and at week 4 of treatment are depicted according to the presence or absence of PLNE in Figure 1. Viral decline between the start of treatment and week 4 was smaller in patients with PLNE than in those without (P = 0.028 by Wilcoxon rank sum test).

Patient characteristics according to the virological responses are shown in Table 2. In six patients, the

Table 1 Patient characteristics according to the presence or absence of PLNE

Parameter	PLNE positive, n = 22	PLNE negative, n = 90	P-value
Age (years)†	60.5 ± 8.8	57.2 ± 8.9	0.12
Male/female	14/8	40/50	0.10
Albumin (g/dL)†	4.01 ± 0.40	4.04 ± 0.33	0.75
AST (U/L)†	62.6 ± 41.2	61.0 ± 38.9	0.87
ALT (U/L)†	76.0 ± 62.2	72.4 ± 56.6	0.81
GGT (U/L)†	37.2 ± 24.6	53.5 ± 39.1	0.018
Alkaline phosphatase (U/L)†	211.7 ± 80.9	199.0 ± 66.3	0.50
Total bilirubin (mg/dL)†	0.82 ± 0.29	0.87 ± 0.47	0.48
Prothrombin time activity (%)	85.8 ± 12.5	85.9 ± 14.7	0.97
AFP (ng/mL)†	22.8 ± 44.0	13.0 ± 21.7	0.32
Liver stiffness (kPa)†	10.8 ± 6.9	12.7 ± 11.9	0.32
Platelet count (×10⁴/μL)†	15.2 ± 8.2	15.5 ± 5.3	0.85
HCV viral load (KIU/mL)‡	731 (358–1070)	636 (151–1045)	0.51
SVR rate (%)§	18.2	41.1	0.045

†Data are presented as mean ± standard deviation, and compared by Student's t-tests.
‡Data are presented as median (25–75% range), and compared by Mann–Whitney U-tests.
§Data are compared by χ²-tests.
AFP, α-fetoprotein; ALT, alanine aminotransferase; AST, aspartate aminotransferase; GGT, γ-glutamyltransferase; HCV, hepatitis C virus; IL, interleukin; PLNE, perihepatic lymph node enlargement; SVR, sustained virological response.

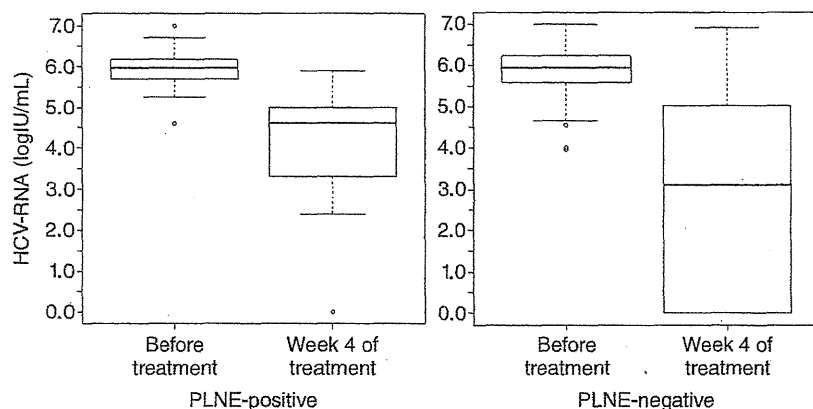© 2013 The Japan Society of Hepatology

Figure 1 Changes in viral load in patients treated by PEG IFN plus RBV according to the presence or absence of PLNE. The viral loads before treatment with PEG IFN plus RBV and at week 4 of treatment were analyzed in patients with PLNE (PLNE positive, *n* = 22) and without PLNE (PLNE negative, *n* = 90). Viral decline was smaller in patients with PLNE than in those without (*P* = 0.028 by Wilcoxon rank sum test). HCV, hepatitis C virus; PEG IFN, pegylated interferon-α; PLNE, perihepatic lymph node enlargement; RBV, ribavirin.

effect of PEG IFN plus RBV therapy was lost during the treatment. Among the three groups of patients divided by the treatment outcome, namely, SVR, relapse or NVR, the rate of PLNE positive patients was least (4/41, 9.8%) in the SVR group (*P* = 0.033). Regarding other parameters, liver stiffness values were lowest (*P* = 0.033) in the SVR group, whereas serum albumin levels were lowest in the NVR group (*P* = 0.004), in line with the well-known evidence that patients with advanced liver fibrosis are difficult to treat with IFN.[20]

Then, the predicting factors for SVR were analyzed, and the results are shown in Table 3. Nine factors that had a *P*-value of less than 0.4 in univariate analysis were subsequently included in multivariate logistic regression analysis. As a result, ALT, GGT, liver stiffness and PLNE were retained as independent predicting factors for SVR (Table 3). These results suggest that the presence of PLNE is a negative predictor for achievement of SVR by PEG IFN and RBV therapy in chronic hepatitis C patients with genotype 1 and HCV RNA of more than 100 KIU/mL, independent of liver fibrosis.

Table 2 Patient characteristics according to the virological responses

Parameter	SVR, *n* = 41	Relapse, *n* = 29	NVR, *n* = 36	*P*-value
Age (years)†	57.3 ± 8.9	57.3 ± 9.1	58.8 ± 8.9	0.71
Male/female§	18/23	16/13	17/19	0.55
Albumin (g/dL)†	4.11 ± 0.28	4.10 ± 0.35	3.87 ± 0.37	0.004
AST (U/L)†	61.2 ± 43.8	56.6 ± 33.9	65.2 ± 34.1	0.67
ALT (U/L)†	81.6 ± 70.6	63.2 ± 40.1	71.4 ± 37.1	0.36
GGT (U/L)†	42.6 ± 30.3	48.5 ± 33.4	62.8 ± 45.6	0.056
Alkaline phosphatase (U/L)†	187.2 ± 73.9	211.7 ± 56.6	203.0 ± 73.7	0.33
Total bilirubin (mg/dL)†	0.78 ± 0.22	0.86 ± 0.32	0.99 ± 0.67	0.11
Prothrombin time (%)†	86.1 ± 17.1	84.8 ± 12.4	87.1 ± 12.3	0.80
AFP (ng/mL)†	9.6 ± 18.5	12.0 ± 27.0	23.2 ± 35.5	0.082
Liver stiffness (kPa)†	8.9 ± 4.7	13.5 ± 11.7	15.4 ± 14.9	0.033
Platelet counts (×10⁴/μL)†	16.1 ± 4.4	16.8 ± 7.7	13.7 ± 5.8	0.077
HCV viral load (KIU/mL)‡	641 (150–1260)	670 (286–1168)	615 (168–951)	0.86
PLNE negative/positive§	37/4	21/8	28/8	0.033
Rate of PLNE positive (%)	9.8	27.6	22.2	

†Data are presented as mean ± standard deviation and compared by Student's *t*-tests.
‡Data are presented as median (25–75% range) and compared by Kruskal–Wallis rank sum tests.
§Data are compared by Fischer's exact tests.
AFP, α-fetoprotein; ALT, alanine aminotransferase; AST, aspartate aminotransferase; GGT, γ-glutamyltransferase; HCV, hepatitis C virus; IL, interleukin; NVR, null virological response; PLNE, perihepatic lymph node enlargement; SVR, sustained virological response.